AIMS Mathematics, 11(4): 10638–10667.
DOI: 10.3934/math.2026438
Received: 13 December 2025
Revised: 28 March 2026
Accepted: 03 April 2026
Published: 20 April 2026

https://www.aimspress.com/journal/Math

Research article

Extropy-based characterization and nonparametric testing of symmetry in continuous distributions via consecutive systems

Tahani Alshathri* **and Mohamed Kayid**

Department of Statistics and Operations Research, College of Science, King Saud University, P.O. Box 2455, Riyadh 11451, Saudi Arabia

* **Correspondence:** Email: 444203975@student.ksu.edu.sa; Tel: +966554409333.

Abstract: This paper develops a unified information-theoretic framework for the characterization of continuous symmetric distributions based on extropy and cumulative extropy measures. The proposed approach is formulated through the structural properties of consecutive $(n-r)$-out-of-n:G and $(n-r)$-out-of-n:F systems, which naturally arise in reliability and lifetime analysis. We establish necessary and sufficient conditions under which the equality of differential extropy, cumulative residual extropy, and cumulative past extropy uniquely characterizes distributional symmetry for all $n \geq 2r$. These results contribute to statistical distribution theory by providing new system-based information characterizations of symmetry. Building on the theoretical developments, we introduce a new nonparametric test for symmetry constructed from differences between estimated extropy measures associated with consecutive systems. The proposed test is shown to be consistent, and extensive Monte Carlo simulations demonstrate that it achieves competitive and often superior power compared with several existing symmetry tests, particularly in detecting mild and near-symmetric departures. Applications to real datasets further confirm the practical effectiveness and interpretability of the proposed methodology. The proposed framework naturally admits extensions in multivariate settings and to other information measures.

Keywords: symmetric distributions; extropy; cumulative extropy; consecutive reliability systems; nonparametric symmetry testing; distribution characterization
Mathematics Subject Classification: 62G10, 94A17, 62E10, 62N05

1. Introduction

Statistical distribution theory forms a cornerstone of modern probability and statistical inference, providing fundamental tools for modeling uncertainty and understanding the structural properties of random phenomena. In particular, the characterization of probability distributions through analytical, probabilistic, or information-theoretic properties has long played a central role in identifying distributional features and developing inference procedures with broad applicability. Recent advances have highlighted the importance of information-based measures in distribution theory, especially in bridging theoretical characterizations with practical statistical applications.

Information-theoretic measures have long been recognized as powerful tools in statistical distribution theory, owing to their ability to capture uncertainty and structural properties of random variables in a concise and model-independent manner. Among these measures, entropy-based quantities have played a central role in both theoretical developments and statistical applications. Shannon entropy is a fundamental concept in information theory that quantifies the uncertainty associated with a random variable X taking values $\{x_1, \dots, x_n\}$ with the probability mass function $\mathbf{q}_n = (q_1, \dots, q_n)$, where $q_i = P(X = x_i)$ and $\sum_{i=1}^{n} q_i = 1$. The Shannon entropy is defined as:

$$\mathcal{H}(\mathbf{q}_n) = -\sum_{i=1}^{n} q_i \log\, q_i,$$

where $\log(\cdot)$ denotes the natural logarithm (Shannon [1]). Recently, Lad et al. [2] introduced extropy as a dual measure of entropy, which is defined by

$$\mathcal{J}(\mathbf{q}_n) = -\sum_{i=1}^{n} (1 - q_i) \log (1 - q_i),$$

which also captures distributional uncertainty but emphasizes complementary probabilistic structure. Although entropy and extropy coincide for binary distributions, they generally differ for higher dimensions. Both measures are maximized by the uniform distribution and are invariant under permutations of the probability mass function; however, they assess distributional refinement in fundamentally different ways. In the continuous setting, uncertainty measures are typically defined through density-based analogs. The continuous counterpart of Shannon entropy, known as *differential entropy*, is given by

$$\mathcal{H}(X) = -\int_{\mathcal{S}_X} f(x) \log f(x)\, dx = -\int_0^1 \log f\big(F^{-1}(u)\big) du, \tag{1}$$

provided the integral exists, where f and F denote the probability density and cumulative distribution functions of X, respectively; $\mathcal{S}_X$ is the support of X; and $F^{-1}(u) = \inf\{x; F(x) \geq u\}$ is the quantile function. Although $\sigma^2(X) < \infty$ implies $\mathbb{E}(|X|) < \infty$ and $\mathcal{H}(X) < \infty$, the converse does not necessarily hold, as illustrated by the Cauchy distribution.

Motivated by Shannon's refinement argument for discrete entropy and its continuous limit, Lad et al. [2] proposed extropy as a complementary uncertainty measure for continuous random variables. Specifically, for large n, extropy admits the approximation

$$\mathcal{J}(\mathbf{q}_n) \approx 1 - \frac{\Delta x}{2} \sum_{i=1}^{n} f^2(x_i) \Delta x,$$

where $\Delta \mathrm{x} = (x_\mathrm{n} - x_1)/(n-1)$. Accordingly, the differential extropy of a continuous random variable with density f is defined as the limit

$$\mathcal{J}(X) = \lim_{\Delta x \to 0} \frac{[J(\mathbf{q}_n) - 1]}{\Delta x} = -\frac{1}{2} \int_{\mathcal{S}_X} f^2(x) dx. \tag{2}$$

Extropy and its statistical applications have attracted considerable attention in recent years. Xiong

et al. [3] (see also Raqab and Qiu [4]) proposed a symmetry test based on the extropy of upper and lower k-record values. Building on this idea, Jose and Sathar [5] investigated extropy associated with the n-th upper and lower k-records under symmetry. More recently, Gupta and Chaudhary [6] employed extropy measures of record values to characterize continuous symmetric distributions.

In a related development, Jahanshahi et al. [7] introduced cumulative residual extropy (CREX) as an alternative uncertainty measure defined by

$$\xi(X) = -\frac{1}{2}\int_{\mathcal{S}_X} \bar{F}^2(x)dx, \tag{3}$$

where $\bar{F}(x) = 1 - F(x)$ denotes the survival function. The main motivation for CREX lies in the greater regularity of the cumulative distribution function compared to the probability density function, the latter being a derivative and often less stable in empirical settings. In many practical reliability problems, it is the probability that a system survives beyond a given time, rather than the probability of failure at an exact time point, that is of primary interest. Consequently, CREX provides a meaningful framework for comparing uncertainty associated with the lifetimes of different systems (see Jahanshahi et al. [7], Remark 2.3). Parallel to CREX, the cumulative past extropy (CPEX) of a random variable X was defined by Gupta and Chaudhary [6] as

$$\bar{\xi}(X) = -\frac{1}{2}\int_{\mathcal{S}_X} F^2(x)dx. \tag{4}$$

Whereas CREX quantifies uncertainty related to the future lifetime of a system, CPEX serves as its dual by capturing uncertainty associated with the past, namely the portion of the lifetime that has already elapsed. Motivated by these developments, this work characterizes continuous symmetric distributions by combining information-theoretic measures with reliability-based system structures. A random variable X is said to have a symmetric distribution about a point μ if its probability distribution is evenly distributed on both sides of μ. Formally, for a random variable with cumulative distribution function F, symmetry can be expressed as

$$F(\mu - x) + F(\mu + x) = 1, x \in \mathcal{S}_X.$$

Common examples of symmetric distributions include the Laplace, uniform, normal, logistic, Cauchy, and Student's *t*-distributions.

Consecutive r-out-of-n systems constitute an important and well-studied class of reliability models. A linear consecutive r-out-of-n:G system functions if at least r consecutive components operate successfully, whereas a consecutive r-out-of-n:F system fails if at least r consecutive components fail. The component lifetimes are assumed to be independent and identically distributed (i.i.d.) random variables. Series and parallel systems arise as special cases when r=1 or $r = n$, respectively. Such systems naturally arise in applications such as oil pipelines and communication networks, where sequential component failures may lead to system failure. The reliability properties of consecutive systems have been extensively investigated; see [8–10] and the references therein.

When $2r \geq n$, elegant closed-form expressions are available for the reliability of linear consecutive r-out-of-n:G and r-out-of-n:F systems. Specifically, if component lifetimes have a cumulative distribution function F, and $T_{r|n:G}$ and $T_{r|n:F}$ denote the lifetimes of the corresponding systems, then according to Eryilmaz [11], the associated survival functions for all $2r \geq n$ are given by

$$\bar{F}_{r|n:G}(x) = (n - r + 1)\bar{F}^r(x) - (n - r)\bar{F}^{r+1}(x), x \in \mathcal{S}_X, \tag{5}$$

and

$$F_{r|n:F}(x) = (n-r+1)F^r(x) - (n-r)F^{r+1}(x), x \in \mathcal{S}_X. \quad (6)$$

This paper investigates the characterization of continuous symmetric distributions by exploiting information-theoretic properties of consecutive systems. Symmetric distributions arise naturally in many theoretical and applied contexts and include the well-known families such as the Student's *t*, uniform, Cauchy, normal, Laplace, and logistic distributions. The Cauchy distribution is frequently encountered in physics, whereas the Laplace and normal distributions are widely used in signal processing and statistical mechanics, respectively (see [12]). The characterization of symmetric distributions has attracted sustained attention in the literature. For instance, Mahdizadeh and Zamanzade [13] proposed a nonparametric estimator for symmetric distribution functions under multistage ranked set sampling. Additional characterization results based on order statistics and record values have been developed by several authors (see [14–16]). Despite these extensive developments, characterizations of symmetric distributions based on information measures derived from consecutive system structures have not yet been explored.

On the other hand, the information-theoretic properties of consecutive systems have been investigated in recent studies. In particular, Kayid and Shrahili [17] examined fractional generalized cumulative residual entropy for consecutive systems, and Kayid and Alshehri [18] studied Shannon differential entropy in this context. However, the use of extropy-based information measures of consecutive systems to characterize symmetry constitutes a novel contribution. The present work aims to fill this gap by developing new system-based characterizations of continuous symmetric distributions using extropy, cumulative residual extropy, and cumulative past extropy within the framework of consecutive reliability systems. The main contributions of this paper can be summarized as follows: (i) the derivation of new extropy-based characterization results for distributional symmetry; (ii) the proposal of a new consistent nonparametric test for symmetry, and (iii) a comprehensive empirical study demonstrating strong finite-sample performance and practical applicability.

Throughout the paper, we frequently work with the $(n-r)$-out-of-n system representation. This choice is motivated by the duality between r-out-of-n and $(n-r)$-out-of-n systems, where the latter corresponds to the complementary system structure. This representation is particularly convenient for the information-theoretic analysis conducted in this work, as cumulative residual and cumulative past extropy measures can be expressed more naturally in terms of system survival and failure behavior. Importantly, this formulation does not entail any loss of generality, because results for r-out-of-n systems can be obtained directly through this dual relationship.

The remainder of this paper is organized as follows. Section 2 presents auxiliary results and establishes extropy-based characterizations of symmetric distributions for consecutive $(n-r)$-out-of-n systems, showing that symmetry is equivalent to the equality of differential extropies of the corresponding $(n-r)$-out-of-n:G and $(n-r)$-out-of-n:F systems for all $n \geq 2r$. Section 3 extends these results to cumulative residual extropy and cumulative past extropy. Section 4 illustrates the theoretical findings through several examples involving common symmetric and asymmetric distributions, including the power, Pareto, Cauchy, normal, Gumbel, arcsine, and logit-normal families. In Section 5, we propose a nonparametric test for symmetry based on differences in estimated extropies of consecutive systems, establish its consistency, compute critical values via Monte Carlo simulation for various sample sizes, and demonstrate its superior power, particularly against mild asymmetries, through extensive comparisons with existing symmetry tests. Applications to real datasets are also presented to highlight the practical usefulness of the proposed approach. Finally, Section 6 concludes the paper.

2. Extropy-based characterization of consecutive systems

In this section, we develop extropy-based characterizations of continuous symmetric distributions by exploiting the structural properties of consecutive systems. Unlike existing characterizations that rely on order statistics or record values, the proposed approach derives symmetry conditions directly from information measures associated with system lifetimes. This perspective provides a natural bridge between information theory and reliability analysis and leads to tractable and interpretable characterization results. To establish the main findings, we first recall two auxiliary lemmas that play a central role in characterizations based on symmetry properties. The first lemma, originally due to Fashandi and Ahmadi [14], provides a necessary and sufficient condition for symmetry expressed in terms of the quantile function. The second lemma follows from the Müntz–Szász theorem (see Kamps [19]) and ensures the completeness of certain functional sequences, which is essential for proving the sufficiency parts of our main results.

Let C_s denote the class of all continuous probability density functions f with support S_X satisfying

$$f(F^{-1}(u)) = f(F^{-1}(1-u)), \text{for almost all } u \in (0,1). \tag{7}$$

Now, consider the following lemma.

Lemma 2.1. If X is an absolutely continuous random variable with a cumulative distribution function F and probability density function f with support $\mathcal{S}_X$, then $f \in \mathcal{C}_s$, if there exists a constant μ such that

$$F(\mu - x) = 1 - F(\mu + x), \text{ for all } x \in \mathcal{S}_X. \tag{8}$$

The next lemma presents an important auxiliary result derived using the Müntz–Szász theorem; see Kamps [19]. The exponent sequence used in the proofs satisfies the standard Müntz–Szász condition, ensuring completeness.

Lemma 2.2. Let $\psi(x)$ be an integrable function on (a,b). If $\int_a^b x^{n_j}\psi(x)dx = 0$ for all $j \geq 1$, where $\{n_j\}_{j\geq 1}$ is a strictly increasing sequence of positive integers with $\sum_{j=1}^{\infty} 1/n_j = \infty$, then $\psi(x) = 0$ almost everywhere on (a,b).

It is worth noting that Lemma 2.2 demonstrates the completeness of the sequence $\{x^{n_1}, x^{n_2}, \dots; 1 \leq n_1 < n_2 < \cdots\}$, a standard result in functional analysis. Hwang and Lin [20] extended the Müntz–Szász theorem to functions of the form $\{\phi^{n_j}(x), n_j \geq 1\}$, where $\phi(x)$ is absolutely continuous and monotonic on (a,b). Let $X_1, X_2, \dots, X_n$ be n i.i.d. continuous random variables with a cumulative distribution function F, probability density function $f(x)$, and support $\mathcal{S}_X$, and let $X_{1:n}, X_{2:n}, \dots, X_{n:n}$ be the corresponding order statistics. Let us consider linear consecutive $(n-r)$-out-of-n:G and $(n-r)$-out-of-n: F systems for all $n \geq 2r$, where $r \in \mathcal{D} = \{0,1,\dots,\lfloor n/2 \rfloor\}$, and $\lfloor \cdot \rfloor$ is the floor function. We denote the lifetimes of these systems by $T_{n-r|n:G}$ and $T_{n-r|n:F}$, respectively. It follows from (5) and (6) that:

$$f_{n-r|n:G}(x) = f(x)\left[a_{r,n}\bar{F}^{n-r-1}(x) - b_{r,n}\bar{F}^{n-r}(x)\right], x \in \mathcal{S}_X \tag{9}$$

and

$$f_{n-r|n:F}(x) = f(x)\left[a_{r,n}F^{n-r-1}(x) - b_{r,n}F^{n-r}(x)\right], x \in \mathcal{S}_X, \tag{10}$$

where $a_{r,n} = (n-r)(r+1)$ and $b_{r,n} = (n-r+1)r$ for all $n \geq 2r$, such that $r \in \mathcal{D}$. Assume

component lifetimes are transformed into i.i.d. uniform random variables $U_j = F(X_j)$ on [0,1] for $j = 1, \cdots, n$. When $r \in \mathcal{D}$, the probability density functions of $U_{n-r|n:G} = F(T_{n-r|n:G})$ and $U_{n-r|n:F} = F(T_{n-r|n:F})$ are given by

$$\rho_{n-r|n:G}(u) = a_{r,n}(1-u)^{n-r-1} - b_{r,n}(1-u)^{n-r}, \text{ for } 0 < u < 1 \tag{11}$$

and

$$\rho_{n-r|n:F}(u) = a_{r,n}u^{n-r-1} - b_{r,n}u^{n-r}, \text{for } 0 < u < 1. \tag{12}$$

The above expressions are derived from the transformation $T_{n-r|n:G} = F^{-1}(U_{n-r|n:G})$ and $T_{n-r|n:F} = F^{-1}(U_{n-r|n:F})$, whose Jacobian is $1/f(F^{-1}(u))$. Then, we have $\rho_{n-r|n:G}(u) = f_{n-r|n:G}(F^{-1}(u))/f(F^{-1}(u))$ and $\rho_{n-r|n:F}(u) = f_{n-r|n:F}(F^{-1}(u))/f(F^{-1}(u))$ for $0 < u < 1$. Applying the extropy transformation formula from (2) to $T_{n-r|n:G} = F^{-1}(U_{n-r|n:G})$ and using the results of Alrewely and Kayid [21], we obtain the extropy of the $(n-r)$-out-of-n:G system,

$$\mathcal{J}(T_{n-r|n:G}) = -\frac{1}{2}\int_0^1 \rho^2_{n-r|n:G}(u) f\big(F^{-1}(u)\big)du, \text{for all } n \geq 2r. \tag{13}$$

The identity from Alomani et al. [22] is obtained by applying analogous arguments to the transformation $T_{n-r|n:F} = F^{-1}(U_{n-r|n:F})$, which is given by

$$\mathcal{J}(T_{n-r|n:F}) = -\frac{1}{2}\int_0^1 \rho^2_{n-r|n:F}(u) f\big(F^{-1}(u)\big)du \text{ for all } n \geq 2r. \tag{14}$$

Now, let us provide an example to illustrate the application of the results presented in the above.

Example 2.1. Consider a random variable X with probability density function $f(x) = bx^{b-1}$ and cumulative distribution function $F(x) = x^b$ for $0 < x < 1$ and $b > 0$. Then, $f(F^{-1}(u)) = bu^{(b-1)/b}$ for $0 < u < 1$. Applying (12) and (13), and using the relation $\rho_{n-r|n:G}(u) = \rho_{n-r|n:F}(1-u)$ for all $0 < u < 1$, we have

$$\begin{aligned}
\mathcal{J}(T_{n-r|n:G}) - \mathcal{J}(T_{n-r|n:F}) &= 0.5\left[\int_0^1 \rho^2_{n-r|n:F}(u) f(F^{-1}(u))du - \int_0^1 \rho^2_{n-r|n:G}(u) f(F^{-1}(u))du\right] \\
&= 0.5b\left[\int_0^1 \rho^2_{n-r|n:F}(u) u^{\frac{b-1}{b}}du - \int_0^1 \rho^2_{n-r|n:G}(u) u^{\frac{b-1}{b}}du\right] \\
&= 0.5b\left[\int_0^1 \rho^2_{n-r|n:F}(u) u^{\frac{b-1}{b}}du - \int_0^1 \rho^2_{n-r|n:F}(1-u) u^{\frac{b-1}{b}}du\right] \\
&= 0.5b\left[\int_0^1 \rho^2_{n-r|n:F}(u)\left(u^{\frac{b-1}{b}} - (1-u)^{\frac{b-1}{b}}\right)du\right],
\end{aligned}$$

where the final equality is obtained by the change of variable $z = 1-u$, followed by renaming z to u. After some manipulations, for all $r \in \mathcal{D}$, we get:

$$\mathcal{J}(T_{n-r|n:G}) - \mathcal{J}(T_{n-r|n:F}) = 0.5b\left[\int_0^{1/2} \left(\rho^2_{n-r|n:F}(u) - \rho^2_{n-r|n:F}(1-u)\right)\left(u^{\frac{b-1}{b}} - (1-u)^{\frac{b-1}{b}}\right)du\right].$$

For $n = 1$ and hence, $r = 0$, we have $\mathcal{J}(T_{n-r|n:G}) - \mathcal{J}(T_{n-r|n:F}) = 0$ for all $r \in \mathcal{D}$. For $n > 1$, if F is symmetric (i.e., $b = 1$), then $\mathcal{J}(T_{n-r|n:G}) - \mathcal{J}(T_{n-r|n:F}) = 0$ for all $r \in \mathcal{D}$. Furthermore, because $\rho_{n-r|n:F}(u)$ is increasing on (0,1/2), it follows that $\rho^2_{n-r|n:F}(u) - \rho^2_{n-r|n:F}(1-u) < 0$ for $0 < u < 1/2$. Consequently, if $b > (<)1$, then $u^{b-1/b} - (1-u)^{b-1/b} < (>)0$ because $0 < u < 1/2 < 1-u < 1$. Therefore, the sign of $\mathcal{J}(T_{n-r|n:G}) - \mathcal{J}(T_{n-r|n:F})$ is determined by the sign of b for all $r \in \mathcal{D}$.

It is worthwhile to note that Example 2.1 demonstrates that the difference $\mathcal{J}(T_{n-r|n:G}) - \mathcal{J}(T_{n-r|n:F})$ may be positive, negative, or zero, depending on the shape of the parent distribution. This observation emphasizes that the equality of extropies is not automatic. The following theorem shows that, under symmetry, this difference vanishes for all $n \geq 2r$, and conversely, that such an equality characterizes symmetry.

Theorem 2.1. Let $X_1, \ldots, X_n$ be i.i.d. continuous random variables with a cumulative distribution function F. Then, F is symmetric if and only if for some fixed but arbitrary $r \in \mathcal{D}, \mathcal{J}(T_{n-r|n:G}) = \mathcal{J}(T_{n-r|n:F})$, for all $n \geq 2r$.

Proof. For the necessity part, assume that F is symmetric about μ (without loss of generality, take $\mu = 0$). Given that $\rho_{n-r|n:G}(u) = \rho_{n-r|n:F}(1-u)$ for all $0 < u < 1$, (12) and (13) imply for a fixed $r \in \mathcal{D}$ that

$$\begin{aligned} -0.5\mathcal{J}(T_{n-r|n:G}) &= \int_0^1 \rho^2_{n-r|n:G}(u) f(F^{-1}(u)) du \\ &= \int_0^1 \rho^2_{n-r|n:F}(1-u) f(F^{-1}(u)) du \\ &= \int_0^1 \rho^2_{n-r|n:F}(z) f(F^{-1}(1-z)) dz, \text{ taking } z = 1-u \\ &= \int_0^1 \rho^2_{n-r|n:F}(z) f\big(F^{-1}(z)\big) dz = -0.5\mathcal{J}(T_{n-r|n:F}), \end{aligned}$$

where the last equality follows from the observation that F is symmetric upon recalling (7), thereby completing the necessity part of the proof. For the sufficiency part, we assume for a fixed $r \in \mathcal{D}$ that $\mathcal{J}(T_{n-r|n:G}) = \mathcal{J}(T_{n-r|n:F})$ for all $n \geq 2r$. Then, from (12) and (13), one can write

$$\begin{aligned} 0 &= \mathcal{J}(T_{n-r|n:G}) - \mathcal{J}(T_{n-r|n:F}) \\ &= \textstyle\int_0^1 \rho^2_{n-r|n:F}(u) f(F^{-1}(u)) du - \int_0^1 \rho^2_{n-r|n:G}(u) f(F^{-1}(u)) du \\ &= \textstyle\int_0^1 \rho^2_{n-r|n:F}(u) f(F^{-1}(u)) du - \int_0^1 \rho^2_{n-r|n:F}(1-u) f(F^{-1}(u)) du \\ &= \textstyle\int_0^1 \rho^2_{n-r|n:F}(u) f(F^{-1}(u)) du - \int_0^1 \rho^2_{n-r|n:F}(z) f(F^{-1}(1-z)) dz, \text{ taking } z = 1-u \\ &= \textstyle\int_0^1 \rho^2_{n-r|n:F}(u) \big[f\big(F^{-1}(u)\big) - f\big(F^{-1}(1-u)\big)\big] du, \text{for all } n \geq 2r. \end{aligned} \tag{14}$$

Consequently, we get

$$\int_0^1 \phi_{r,n}(u) \big[f\big(F^{-1}(u)\big) - f\big(F^{-1}(1-u)\big)\big] u^{n-2r} du = 0,$$

where $\phi_{r,n}(u) = \big(a_{r,n} u^{-1} - b_{r,n}\big)^2$ for $0 < u < 1$. By applying Lemma 2.2 with the function

$$\psi(u) = \phi_{r,n}(u) \big[f\big(F^{-1}(u)\big) - f\big(F^{-1}(1-u)\big)\big]$$

and noting that $\{u^{n-2r}, n \geq 2r\}$ is the complete sequence, we conclude that $f(F^{-1}(u)) = f(F^{-1}(1-u))$ a.s. for all $0 < u < 1$, which means that $f \in \mathcal{C}_s$. The proof is then completed by Lemma 2.1. ■

The equality of the two system-based extropy measures can be understood as a balance between failure patterns observed from the left and the right of the distribution. The consecutive $(n-r)$-out-of-n:G structure emphasizes survival configurations, whereas the corresponding $(n-r)$-out-of-n:F

system reflects failure accumulation. If the underlying distribution is symmetric, the probabilistic weight assigned to configurations at a distance d to the left of the center must coincide with the weight assigned at the same distance to the right. Consequently, both systems transmit identical amounts of uncertainty, leading to equal extropy values. Conversely, any systematic deviation from mirror behavior produces an imbalance in how survival and failure information accumulate, and this discrepancy is captured immediately through unequal extropy measures. Hence, equality naturally encodes symmetry.

Remark 2.1. Under the conditions of Theorem 2.1, if $\mathcal{J}(T_{n-r|n:G}) - \mathcal{J}(T_{n-r|n:F}) = d$ for all $n \geq 2r$, with d constant with respect to n, then, as in the proof of Theorem 2.1, we have

$$F\big(a(\mu - x)\big) + F(\mu + x) = 1, \text{for all } x \in R, \tag{15}$$

where $a = e^d > 0$. For $a = 1$, F is symmetric; otherwise, (15) defines a family of asymmetric distributions. This remark shows that departures from symmetry can be explicitly characterized through constant extropy differences. Here, a question can arise: If $\mathcal{J}(T_{n-r|n:G}) = \mathcal{J}(T_{n-r|n:F})$ only for a specific r and n, does F necessarily possess symmetry? To explore this, we begin by considering the case where $r = 0$.

Theorem 2.2. Under the assumptions of Theorem 2.1, the following are equivalent:
(i) F has a symmetric distribution;
(ii) $f \in C_s$ and $\mathcal{J}(T_{n|n:G}) = \mathcal{J}(T_{n|n:F})$ for fixed $n \geq 1$.

Proof. The implication (i) $\Longrightarrow$ (ii) is clear. Conversely, suppose $\mathcal{J}(T_{n|n:G}) = \mathcal{J}(T_{n|n:F})$ for some fixed $n \geq 1$. Then, from (12) and (13), we have

$$\int_0^1 (1-u)^{2(n-1)} f\big(F^{-1}(u)\big)du = \int_0^1 u^{2(n-1)} f\big(F^{-1}(u)\big)du.$$

Substituting $z = 1 - u$ into the left-hand side of the above relation yields

$$\int_0^1 z^{2(n-1)}[f(F^{-1}(z)) - f(F^{-1}(1-z))]dz = 0,$$

or equivalently,

$$\int_0^{1/2} \left[z^{2(n-1)} - (1-z)^{2(n-1)}\right][f(F^{-1}(z)) - f(F^{-1}(1-z))]dz = 0. \tag{16}$$

Given that $n \geq 1$, we have $0 < z^{2(n-1)} < (1-z)^{2(n-1)} < 1$, over $z \in (0,1/2)$ because $0 < u < 1/2 < 1 - u < 1$. Consequently, the first term within the brackets of the integrand in (16) becomes negative. So, for almost all $z \in (0,1/2)$, it holds that $f(F^{-1}(z)) = f(F^{-1}(1-z)$, as $f \in \mathcal{C}$ by assumption. The proof is finalized by applying Lemma 2.1. ■

In the following theorem, we demonstrate that the same results hold as in the previous theorem for the case where $r \in D \setminus 0 = \{1, \ldots, \lfloor n/2 \rfloor\}$.

Theorem 2.3. Under the assumptions of Theorem 2.1, the following are equivalent:
(i) F has a symmetric distribution;
(ii) $f \in \mathcal{C}$ and $\mathcal{J}(T_{n-r|n:G}) = \mathcal{J}(T_{n-r|n:F})$ for some $n, (n \geq 2r)$ and a fixed $r \in D \setminus 0$.

Proof. We prove only that (ii) implies (i), because the converse follows directly from Theorem 2.1. Assume there exists some $n > 1$ and a fixed $r \in D \setminus \{0\}$ such that $\mathcal{J}(T_{n-r|n:G}) = \mathcal{J}(T_{n-r|n:F})$. Then, Eq (14) implies that

$$\int_0^1 \rho_{n-r|n:F}^2(z)\left[f\left(F^{-1}(z)\right)-f\left(F^{-1}(1-z)\right)\right]dz=0,$$

which can be rewritten as follows:

$$\int_0^{1/2}\left[\rho_{n-r|n:F}^2(z)-\rho_{n-r|n:F}^2(1-z)\right]\left[f(F^{-1}(z))-f(F^{-1}(1-z))\right]dz=0. \tag{17}$$

To determine the sign of the integrand in (17), we examine the monotonicity of the function

$$\rho_{n-r|n:F}(z)=a_{r,n}z^{n-r-1}-b_{r,n}z^{n-r}, \text{ for } z\in(0,1/2) \text{ and } r\in D\setminus 0.$$

The derivative of this function is

$$\rho'_{n-r|n:F}(z)=(n-r)z^{n-r-2}[(n-r-1)(r+1)-r(n-r+1)z].$$

For $1\le r\le\lfloor n/2\rfloor$, we have $\rho'_{n-r|n:F}(z)>0$ for all $z<z_r$, where $z_r=(n-r-1)(r+1)/r(n-r+1)$. Because z_r decreases with r, then $\rho_{n-r|n:F}(z)$ increases for $z<z_{\lfloor n/2\rfloor}$. If n is even, let $n=2m$ for some integer $m\ge 1$. Then, $\lfloor n/2\rfloor=m$, and hence, $z_m=1-(1/m)$. By noting that $n=2m$, we have $1/m=2/n$, so $z_{\lfloor n/2\rfloor}=1-2/n$. If n is odd, let $n=2m+1$ for some integer $m\ge 1$. Similarly, one can obtain $z_{\lfloor n/2\rfloor}=1-2/(n+1)$. Hence, because $z_{\lfloor n/2\rfloor}=1-2/n$ for even n, and $z_{\lfloor n/2\rfloor}=1-2/(n+3)$ for odd n, we have $z_{\lfloor n/2\rfloor}>0.5$ in both cases. Thus, $\rho_{n-r|n:F}(z)$ is increasing over $z\in(0,1/2)$ for $1\le r\le\lfloor n/2\rfloor$. From $0<z<1/2<1-z<1$, it follows that $\rho_{n-r|n:F}^2(z)<\rho_{n-r|n:F}^2(1-z)$ for all $0<z<1/2$ and $r\in D\setminus 0$. Consequently, the first term in the brackets of the integrand (17) is negative, implying $f(F^{-1}(z))=f(F^{-1}(1-z))$ for almost all $z\in(0,1/2)$, given $f\in\mathcal{C}$. Thus, Lemma 2.1 completes the proof. ■

3. Cumulative extropies characterization of consecutive systems

In this section, we extend the extropy-based characterizations developed in Section 2 to CREX and CPEX. Unlike differential extropy, these cumulative measures depend on the distribution function rather than the density, which provides additional robustness and interpretability in reliability and lifetime analysis. We show that symmetry can be equivalently characterized through the equality of CREX and CPEX associated with consecutive systems, thereby demonstrating that the proposed characterization framework is stable across different classes of information measures. To this end, we first derive explicit expressions for the CREX and CPEX of consecutive $(n-r)$-out-of-n:G and $(n-r)$-out-of-n:F systems. Assuming $r\in\mathcal{D}$, the survival function of $U_{n-r|n:G}=F(T_{n-r|n:G})$ and the cumulative distribution function of $U_{n-r|n:F}=F(T_{n-r|n:F})$ for $0<u<1$ are given by

$$\bar{Q}_{n-r|n:G}(u)=(r+1)(1-u)^{n-r}-r(1-u)^{n-r+1}, \tag{18}$$

and

$$Q_{n-r|n:F}(u)=(r+1)u^{n-r}-ru^{n-r+1}. \tag{19}$$

By using the change of variable $u=F(x)$, we can get

$$\xi(T_{n-r|n:G})=-\frac{1}{2}\int_{S_X}\bar{F}_{n-r|n:G}^2(x)dx=-\frac{1}{2}\int_0^1\frac{\bar{Q}_{n-r|n:G}^2(u)}{f(F^{-1}(u))}du. \tag{20}$$

These representations mirror those obtained for differential extropy, with the key difference that the density function is replaced by the distribution function. The same results also hold for the consecutive

$(n-r)$-out-of-n: F system; that is, one can write

$$\bar{\xi}(T_{n-r|n:F}) = -\frac{1}{2}\int_{S_X} F^2_{n-r|n:F}(x)dx = -\frac{1}{2}\int_0^1 \frac{Q^2_{n-r|n:F}(u)}{f(F^{-1}(u))}du. \tag{21}$$

The following theorem demonstrates that the equality of the CREX of $T_{n-r|n:G}$ and CPEX of $T_{n-r|n:F}$ is a characteristic property of symmetric distributions.

Theorem 3.1. Let $X_1, \ldots, X_n$ be i.i.d. continuous random variables with $CDF F$. Then, F is symmetric if and only if, for a fixed value $r \in \mathcal{D}, \xi(T_{n-r|n:G}) = \bar{\xi}(T_{n-r|n:F})$ for all $n \geq 2r$.

Proof. For the necessity part, because $f \in \mathcal{C}_s$, consider a symmetric distribution centered around μ (assume $\mu = 0$ without loss of generality). Given that $\bar{Q}_{n-r|n:G}(u) = Q_{n-r|n:F}(1-u)$ for all $0 < u < 1$, Eqs (20) and (21) imply for a fixed $r \in \mathcal{D}$ that

$$\begin{aligned} -0.5\xi(T_{n-r|n:G}) &= \int_0^1 \frac{\bar{Q}^2_{n-r|n:G}(u)}{f(F^{-1}(u))}du = \int_0^1 \frac{Q^2_{n-r|n:F}(1-u)}{f(F^{-1}(u))}du \\ &= \int_0^1 \frac{Q^2_{n-r|n:F}(z)}{f(F^{-1}(1-z))}dz = \int_0^1 \frac{Q^2_{n-r|n:F}(z)}{f(F^{-1}(z))}dz \\ &= -0.5\bar{\xi}(T_{n-r|n:F}), \end{aligned}$$

where the third equality is obtained from the change of variable $z = 1-u$, and the last equality follows from the observation that F is symmetric upon recalling (7), thereby completing the necessity part of the proof. For the sufficiency part, we assume for a fixed $r \in \mathcal{D}$ that $\xi(T_{n-r|n:G}) = \bar{\xi}(T_{n-r|n:F})$ for all $n \geq 2r$. Then, from Eqs (20) and (21), one can write

$$\begin{aligned} 0 &= \xi(T_{n-r|n:G}) - \bar{\xi}(T_{n-r|n:F}) \\ &= \int_0^1 \frac{Q^2_{n-r|n:F}(u)}{f(F^{-1}(u))}du - \int_0^1 \frac{\bar{Q}^2_{n-r|n:F}(u)}{f(F^{-1}(u))}du \\ &= \int_0^1 \frac{Q^2_{n-r|n:F}(u)}{f(F^{-1}(u))}du - \int_0^1 \frac{Q^2_{n-r|n:F}(1-u)}{f(F^{-1}(u))}du \\ &= \int_0^1 \frac{Q^2_{n-r|n:F}(u)}{f(F^{-1}(u))}du - \int_0^1 \frac{Q^2_{n-r|n:F}(z)}{f(F^{-1}(1-z))}dz \\ &= \int_0^1 Q^2_{n-r|n:F}(u)\left[\frac{1}{f(F^{-1}(u))} - \frac{1}{f(F^{-1}(1-u))}\right]du, \text{for all } n \geq 2r. \end{aligned} \tag{22}$$

Consequently, we get

$$\int_0^1 \omega_{r,n}(u)\left[\frac{1}{f(F^{-1}(u))} - \frac{1}{f(F^{-1}(1-u))}\right]u^{n-2r}du = 0,$$

where $\omega_{r,n}(u) = ((r+1) - ru)^2$, for $0 < u < 1$. By applying Lemma 2.2 with the function

$$\psi(u) = \omega_{r,n}(u)\left[\frac{1}{f\left(F^{-1}(u)\right)} - \frac{1}{f\left(F^{-1}(1-u)\right)}\right],$$

and noting that $\{u^{n-2r}, n \geq 2r\}$ is the complete sequence, we conclude that $f(F^{-1}(u)) = f(F^{-1}(1-u))$ a.s. for all $0 < u < 1$, which means that $f \in \mathcal{C}_s$. The proof is then completed by Lemma 2.1. ■

The results of Theorem 2.3 extend naturally to the class of cumulative entropies, as stated in the following theorem.

Theorem 3.2. Let $X_1, \ldots, X_n$ be i.i.d. continuous random variables with cumulative distribution function F. The following are equivalent:
(i) F has a symmetric distribution;
(ii) $f \in \mathcal{C}_s$ and $\xi(T_{n|n:G}) = \bar{\xi}(T_{n|n:F})$ for a fixed value $n \geq 1$.

Proof. Because the demonstration of (i) to (ii) is straightforward; we show that (ii) implies (i). Conversely, assume that $\xi(T_{n|n:G}) = \bar{\xi}(T_{n|n:F})$ for a fixed value $n \geq 1$. Then,

$$\int_0^1 \frac{(1-u)^2}{f(F^{-1}(u))}\,du = \int_0^1 \frac{u^2}{f(F^{-1}(u))}\,du.$$

The substitution $z = 1-u$ yields

$$\int_0^1 z^2 \left[\frac{1}{f(F^{-1}(z))} - \frac{1}{f(F^{-1}(1-z))}\right] dz = 0,$$

which is equivalent to

$$\int_0^{1/2} [z^2 - (1-z)^2] \left[\frac{1}{f(F^{-1}(z))} - \frac{1}{f(F^{-1}(1-z))}\right] dz = 0.$$

Because $n \geq 1$, we have $0 < z^2 < (1-z)^2 < 1$ for $z \in (0,1/2)$. Therefore, the first term in the integrand is negative. Consequently, because $f \in \mathcal{C}_s$, it holds that $f(F^{-1}(z)) = f(F^{-1}(1-z))$ for almost all $z \in (0,1/2)$. Thus, Lemma 2.1 completes the proof. ■

The following theorem extends the results of the previous theorem to the case where $r \in \{1, \ldots, \lfloor n/2 \rfloor\}$.

Theorem 3.3. Suppose that the assumptions of Theorem 2.1 hold. Then, the following two statements are equivalent:
(i) F has a symmetric distribution;
(ii) $f \in \mathcal{C}_s$ and $\xi(T_{n-r|n:G}) = \bar{\xi}(T_{n-r|n:F})$ for some n, $(n \geq 2)$, and fixed value $r \in D \setminus 0$.

Proof. Because the demonstration of (i) to (ii) is straightforward, we show that (ii) implies (i). Assume there exists $n \geq 2$ and fixed value $r \in D \setminus \{0\}$ such that $\xi(T_{n-r|n:G}) = \bar{\xi}(T_{n-r|n:F})$. From (22), we have

$$\int_0^1 Q^2_{n-r|n:F}(u) \left[\frac{1}{f\left(F^{-1}(u)\right)} - \frac{1}{f\left(F^{-1}(1-u)\right)}\right] du = 0,$$

which can be rewritten as

$$\int_0^{1/2} \left[Q^2_{n-r|n:F}(z) - Q^2_{n-r|n:F}(1-z)\right] \left[\frac{1}{f(F^{-1}(z))} - \frac{1}{f(F^{-1}(1-z))}\right] dz = 0. \tag{23}$$

Because $Q_{n-r|n:F}(z)$ is increasing for $z \in (0,1/2)$ with fixed $r \in D \setminus \{0\}$, it follows that $Q^2_{n-r|n:F}(z) - Q^2_{n-r|n:F}(1-z) < 0$ for $0 < z < 1/2 < 1-z < 1$. Thus, the negativity of the first term in the brackets of the integrand in (23), combined with the fact that $f \in \mathcal{C}$, implies $f(F^{-1}(z)) = f(F^{-1}(1-z))$ for almost all $z \in (0,1/2)$. The proof is then completed by Lemma 2.1. ■

4. Illustrative examples of symmetry and asymmetry

To illustrate the extropy- and cumulative -extropy-based characterizations developed in Sections 2

and 3, we examine several widely used continuous distributions exhibiting symmetry or controlled asymmetry. These examples demonstrate the ability of the proposed criteria to distinguish between symmetric and asymmetric distributions under varying parameter settings and to clarify the sign and behavior of extropy and cumulative extropy differences associated with consecutive systems. The selected distributions span a range of shapes commonly encountered in applied probability, reliability theory, and statistical modeling, including families that smoothly transition from symmetry to asymmetry through a single parameter. Collectively, the examples highlight the sensitivity and interpretability of the proposed framework and provide a natural bridge to the nonparametric symmetry test introduced in the subsequent section. For further applications in physics, see Kon [23], Naudts [24], and Širca [25]. The nonemptiness of class C_s, including distributions such as the Cauchy, Gumbel, arcsine, power, Pareto, logit-normal, and standard normal, is discussed in Ahmadi [26]. These examples also provide intuition for the behavior of the proposed test statistic.

The following example demonstrates that the proposed extropy- and cumulative extropy-based characterizations not only detect symmetry but also correctly identify the direction of asymmetry in the underlying distribution.

Example 4.1. Following Example 2.1, we have $f(F^{-1}(u)) = bu^{(b-1)/\mathrm{b}}$ and $f(F^{-1}(1-u)) = b(1-u)^{(b-1)/\mathrm{b}}$ for $0 < u < 1$. For $u \in (0, 1/2)$, we have $f(F^{-1}(u)) < f(F^{-1}(1-u))$ if $b > 1$, $f(F^{-1}(u)) > f(F^{-1}(1-u))$ if $b < 1$, and $f(F^{-1}(u)) = f(F^{-1}(1-u))$ if $b = 1$. Thus, the power distribution belongs to class C_s. By Theorem 2.3, we get

$$\begin{aligned}\mathcal{J}(T_{n-r|n:G}) - \mathcal{J}(T_{n-r|n:F}) &= \frac{1}{2}\left[\int_0^{1/2} \left(\rho^2_{n-r|n:F}(u) - \rho^2_{n-r|n:F}(1-u)\right)[f(F^{-1}(u)) - f(F^{-1}(1-u))]du\right] \\ &= \frac{1}{2}b\left[\int_0^{1/2} \left(\rho^2_{n-r|n:F}(u) - \rho^2_{n-r|n:F}(1-u)\right)\left[u^{\frac{b-1}{b}} - (1-u)^{\frac{b-1}{b}}\right]du\right],\end{aligned}$$

for some $n(n \geq 2r)$ and a fixed $r \in D \setminus 0$. Given that $\rho^2_{n-r|n:F}(u) - \rho^2_{n-r|n:F}(1-u) < 0$, for all $0 < u < 1/2$ and $r \in D \setminus 0$, we obtain

$$\mathcal{J}(T_{n-r|n:G}) - \mathcal{J}(T_{n-r|n:F}) \begin{cases} < 0 & \text{if } 0 < b < 1 \\ = 0 & \text{if } b = 1 \\ > 0 & \text{if } b > 1. \end{cases}$$

The reason for this is that the power function distribution exhibits asymmetry when $0 < b < 1$ and $b > 1$. Likewise, regarding Theorem 3.3, based on (23), we conclude that

$$\begin{aligned}\xi(T_{n-r|n:G}) - \bar{\xi}(T_{n-r|n:F}) &= \frac{1}{2}\int_0^{1/2} \left[Q^2_{n-r|n:F}(u) - Q^2_{n-r|n:F}(1-u)\right]\left[\frac{1}{f(F^{-1}(u))} - \frac{1}{f(F^{-1}(1-u))}\right]du \\ &= \frac{1}{2}b\int_0^{1/2} \left[Q^2_{n-r|n:F}(u) - Q^2_{n-r|n:F}(1-u)\right]\left[\frac{1}{u^{\frac{b-1}{b}}} - \frac{1}{(1-u)^{\frac{b-1}{b}}}\right]du.\end{aligned}$$

Since $Q^2_{n-r|n:F}(u) < Q^2_{n-r|n:F}(1-u)$ for all $0 < u < 1/2$ and $r \in D \setminus \{0\}$, we have

$$\xi(T_{n-r|n:G}) - \bar{\xi}(T_{n-r|n:F}) \begin{cases} > 0 & \text{if } 0 < b < 1 \\ = 0 & \text{if } b = 1 \\ < 0 & \text{if } b > 1, \end{cases}$$

which means the asymmetry of power function distribution when $0 < b < 1,$ and $b > 1$.

The following example considers the Pareto distribution to illustrate a fundamentally different type of asymmetry from that observed in Example 4.1. In contrast to distributions whose asymmetry

changes with parameter values, the Pareto distribution exhibits an inherent and directionally fixed asymmetry for all admissible parameter choices. This example demonstrates that the proposed extropy- and cumulative -extropy-based characterizations consistently detect such intrinsic asymmetry and produce a stable sign of the associated differences.

Example 4.2. For a Pareto distribution with probability density function $f(x) = bx^{-b-1}$ and cumulative distribution function $F(x) = 1 - x^{-b}$ for $x > 1$ and $b > 0$, we have $f(F^{-1}(u)) = b(1-u)^{(b+1)/\mathrm{b}}$ and $f(F^{-1}(1-u)) = bu^{(b+1)/\mathrm{b}}$ for $0 < u < 1$. Because $f(F^{-1}(u)) > f(F^{-1}(1-u))$ for $u \in (0,1/2)$, and all $b > 0$, the Pareto distribution belongs to class C_s. Therefore, by Theorem 2.3, we have

$$\mathcal{J}(T_{n-r|n:G}) - \mathcal{J}(T_{n-r|n:F}) = 0.5b \int_0^{\frac{1}{2}} \left[\rho^2_{n-r|n:F}(u) - \rho^2_{n-r|n:F}(1-u)\right] \left[(1-u)^{\frac{b+1}{b}} - u^{\frac{b+1}{b}}\right] du,$$

for some $n(n \geq 2r)$ and a fixed $r \in D \setminus \{0\}$. Because $\rho^2_{n-r|n:F}(u) - \rho^2_{n-r|n:F}(1-u) < 0$ for a fixed $r \in D \setminus 0$, and $(1-u)^{(b+1)/\mathrm{b}} - u^{(b+1)/\mathrm{b}} > 0$, for all $0 < u < 1/2$, we find that $\mathcal{J}(T_{n-r|n:G}) - \mathcal{J}(T_{n-r|n:F}) < 0$ for all $b > 0$, reflecting the asymmetry of the Pareto distribution. Furthermore, Theorem 3.3 implies, via Eq (23), that

$$\xi(T_{n-r|n:G}) - \bar{\xi}(T_{n-r|n:F}) = 0.5b \int_0^{\frac{1}{2}} \left[Q^2_{n-r|n:F}(u) - Q^2_{n-r|n:F}(1-u)\right] \left[\frac{1}{(1-u)^{\frac{b+1}{b}}} - \frac{1}{u^{\frac{b+1}{b}}}\right] du,$$

for some $n(n \geq 2r)$ and a fixed $r \in D \setminus \{0\}$. Applying similar arguments as in Example 4.1, we get $\xi(T_{n-r|n:G}) - \bar{\xi}(T_{n-r|n:F}) > 0$, reflecting the asymmetry of the Pareto distribution.

The following example considers a symmetric distribution with heavy tails to illustrate that the proposed extropy- and cumulative extropy-based characterizations correctly yield equality of the corresponding measures in the presence of exact symmetry, even when standard moment-based approaches are not applicable.

Example 4.3. Consider a Cauchy distribution with a probability density function $f(x) = 1/(1+x^2)$ and cumulative distribution function $F(x) = 1/2 + 1/\pi \arctan(x)$ for $x \in \mathbb{R}$. It is straightforward to derive the inverse cumulative distribution function as

$$F^{-1}(u) = \tan\left(\pi u - \frac{\pi}{2}\right) = -\cot(\pi u), \text{for } 0 < u < 1.$$

Notably, because $\cot(\pi(1-u)) = -\cot(\pi u)$, we can express the probability density function at the inverse cumulative distribution function as follows:

$$f(F^{-1}(u)) = f(F^{-1}(1-u)) = \frac{1}{1 + \cot^2(\pi u)}, \text{for } 0 < u < 1.$$

This example confirms that the proposed characterization criteria correctly identify exact symmetry, even for heavy-tailed distributions without finite moments.

The following example considers the normal distribution as a classical symmetric model with finite moments, illustrating that the proposed characterization criteria consistently identify symmetry across both heavy-tailed and light-tailed distributional settings.

Example 4.4. Consider a normal distribution with a probability density function $f(x) = (1/\sqrt{2\pi\sigma^2})exp\left(-\frac{(x-\mu)^2}{2\sigma^2}\right)$, and cumulative distribution function $F(x) = 1/2 + 1/2\,\mathrm{erf}[(x-\mu)/$

$\sigma\sqrt{2}\big]$ for $x \in \mathbb{R}$. It is well known that the inverse cumulative distribution function of the normal distribution is given by

$$F^{-1}(u) = \mu + \sigma\sqrt{2}\text{erf}^{-1}(2u-1), \text{for } 0 < u < 1.$$

Because the error function erf (x) is odd, its inverse is also odd, and thus, $F^{-1}(1-u) = \mu - \sigma\sqrt{2}\text{erf}^{-1}(2u-1)$ for $0 < u < 1$. Consequently, the probability density function evaluated at the quantiles satisfies

$$f(F^{-1}(u)) = f(F^{-1}(1-u)) = \frac{1}{\sqrt{2\pi\sigma^2}} e^{-\left(\text{erf}^{-1}(2u-1)\right)^2}, \text{ for } 0 < u < 1.$$

This example confirms that the proposed characterization criteria correctly identify symmetry for classical distributions with finite moments.

The following example considers the Gumbel distribution as a representative extreme-value model to illustrate how the proposed characterization criteria capture asymmetric behavior commonly encountered in reliability and risk analysis, and to visually support the analytical findings.

Example 4.5. For a Gumbel distribution (also known as the type-I generalized extreme value distribution) with probability density function $f(x) = e^{-(x+e^{-x})}$ and cumulative distribution function $F(x) = e^{-e^{-x}}$ for $-\infty < x < \infty$, we have $f(F^{-1}(u)) = u(-\log(u))$ and $f(F^{-1}(1-u)) = (1-u)(-\log(1-u))$ for $0 < u < 1$. Because $f(F^{-1}(u)) > f(F^{-1}(1-u))$ for $u \in (0,1/2)$, the Gumbel distribution is in class C_s; see Figure 1. Thus, by Theorem 2.3, we have

$$\mathcal{J}(T_{n-r|n:G}) - \mathcal{J}(T_{n-r|n:F})$$

$$= 0.5b \int_0^{1/2} \left[\rho^2_{n-r|n:F}(u) - \rho^2_{n-r|n:F}(1-u)\right][u(-\log(u)) - (1-u)(-\log(1-u))]du,$$

for some $n(n \geq 2r)$ and a fixed $r \in D \setminus \{0\}$. Because $\rho^2_{n-r|n:F}(u) - \rho^2_{n-r|n:F}(1-u) < 0$ for a fixed $r \in D \setminus 0$, and $u(-\log(u)) - (1-u)(-\log(1-u)) > 0$, for all $0 < u < 1/2$, we find that $\mathcal{J}(T_{n-r|n:G}) - \mathcal{J}(T_{n-r|n:F}) < 0$. Furthermore, Theorem 3.3 implies, via (23), that

$$\xi(T_{n-r|n:G}) - \bar{\xi}(T_{n-r|n:F})$$

$$= 0.5b \int_0^{1/2} \left[\rho^2_{n-r|n:F}(u) - \rho^2_{n-r|n:F}(1-u)\right]\left[\frac{1}{u(-\log(u))} - \frac{1}{(1-u)(-\log(1-u))}\right]du,$$

for some $n\,(n \geq 2r)$ and a fixed $r \in D \setminus \{0\}$. Consequently, this implies that $\xi(T_{n-r|n:G}) < \bar{\xi}(T_{n-r|n:F})$, reflecting the asymmetry of the Gumbel distribution.

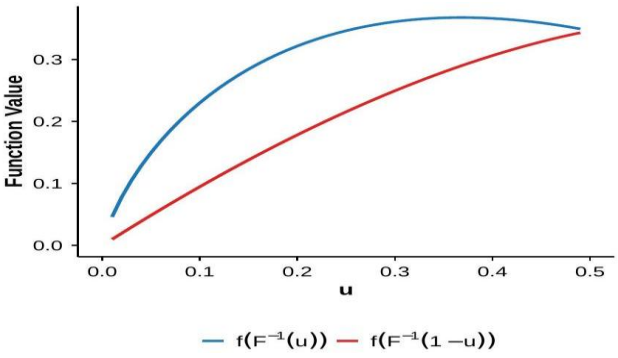

Figure 1. The plot of $f(F^{-1}(u))$ and $f(F^{-1}(1-u))$ for the Gumbel distribution given in Example 4.5.

The following example considers a symmetric distribution with bounded support to illustrate that the proposed characterization criteria remain valid regardless of whether the underlying distribution is supported on a finite or infinite interval.

Example 4.6. Consider an arcsine distribution with probability density function $f(x) = 1/\left[\pi\sqrt{x(1-x)}\right]$ and a cumulative distribution function $F(x) = 2/\pi \arcsin(\sqrt{x})$ for $x \in (0,1)$. It is straightforward to derive the inverse cumulative distribution function as

$$F^{-1}(u) = \sin^2\left(\frac{\pi}{2}u\right), \text{and } F^{-1}(1-u) = \sin^2\left(\frac{\pi}{2}(1-u)\right) = \cos^2\left(\frac{\pi}{2}u\right) \text{for } 0 < u < 1.$$

Notably, we can express the probability density function at the inverse cumulative distribution function as follows:

$$f(F^{-1}(u)) = f(F^{-1}(1-u)) = \frac{1}{\pi \sin\left(\frac{\pi}{2}u\right)\cos\left(\frac{\pi}{2}u\right)}, \text{for } 0 < u < 1.$$

This example confirms that the proposed characterization criteria correctly identify symmetry for distributions with bounded support.

The following example illustrates a symmetric distribution obtained through a nonlinear transformation, demonstrating that the proposed characterization criteria are invariant under transformation-induced symmetry and correctly identify symmetry in the original sample space.

Example 4.7. Let $\text{logit(x)} = \log[\text{x}/(1-\text{x})]$. Consider the logit-normal distribution with probability density function

$$f(x) = \frac{1}{\sqrt{2\pi}}\frac{1}{x(1-x)}e^{-\frac{(\text{logit(x)})^2}{2}} = \frac{\phi\big(\text{logit(x)}\big)}{x(1-x)},$$

and cumulative distribution function F

$$F(x) = \frac{1}{2}\left[1 + \text{erf}\left(\frac{\text{logit(x)}}{\sqrt{2}}\right)\right] = \Phi\big(\text{logit(x)}\big), \text{for } 0 < x < 1,$$

where $\phi(x)$ and $\Phi(\cdot)$ are the probability distribution function and cumulative distribution function of the standard normal distribution, respectively. The inverse cumulative distribution function (quantile function) is obtained by inverting $u = \Phi(\text{logit(x)})$, yielding

$$F^{-1}(u) = \frac{1}{1+e^{-\Phi^{-1}(u)}}, \text{and } F^{-1}(1-u) = \frac{1}{1+e^{-\Phi^{-1}(1-u)}}, \text{for } 0 < u < 1.$$

Thus, for $0 < u < 1$, we obtain:

$$f(F^{-1}(u)) = \frac{\phi(\Phi^{-1}(u))}{F^{-1}(u)(1-F^{-1}(u))}, \text{and } f(F^{-1}(1-u)) = \frac{\phi(\Phi^{-1}(1-u))}{F^{-1}(1-u)(1-F^{-1}(1-u))}.$$

Because the normal distribution is symmetric, we have $\Phi^{-1}(1-u) = -\Phi^{-1}(u)$, and hence, $\phi(\Phi^{-1}(u)) = \phi(\Phi^{-1}(1-u))$ for $0 < u < 1$, because $\phi(-z) = \phi(z)$. Moreover, $\Phi^{-1}(1-u) = -\Phi^{-1}(u)$ implies

$$F^{-1}(1-u)=\frac{1}{1+e^{-\Phi^{-1}(1-u)}}=\frac{1}{1+e^{\Phi^{-1}(u)}}$$
$$=\frac{e^{-\Phi^{-1}(u)}}{1+e^{-\Phi^{-1}(u)}}=1-F^{-1}(u),$$

for $0<u<1$. Consequently, the probability density function evaluated at the quantiles satisfies $f(F^{-1}(u))=f(F^{-1}(1-u))$ for $0<u<1$. This example highlights the ability of the proposed characterization criteria to detect symmetry arising from nonlinear transformations. In addition, symmetry is most naturally understood on the logit scale: If Y is symmetric about its center, then X=logistic(Y) reflects a transformed symmetry pattern on (0,1) induced by the monotone logistic map. We have added this clarification to make the symmetry center and transformation argument explicit.

The illustrative examples presented in this section collectively demonstrate the versatility and robustness of the proposed extropy- and cumulative -extropy-based characterization framework. Through a diverse set of distributions, including models with parameter-dependent asymmetry, inherently asymmetric distributions, and symmetric distributions with heavy tails, light tails, bounded support, and transformation-induced symmetry, the examples confirm that the proposed criteria consistently distinguish between symmetry and asymmetry and accurately reflect the direction of skewness when present. These findings underscore the broad applicability of the characterization results across different distributional structures and provide strong motivation for the nonparametric symmetry test developed in the subsequent section.

5. Test for symmetry

This section proposes a nonparametric goodness-of-fit test for assessing symmetry of an absolutely continuous distribution, directly motivated by the characterization results established in Sections 2–4. The test is designed to detect departures from symmetry without relying on moment assumptions or parametric modeling. Importantly, the proposed test statistic is constructed from order statistics and spacing-type quantities and is therefore invariant under location shifts. Consequently, symmetry about an unknown center does not require explicit estimation of the center parameter. Scale effects, however, influence the variability of the statistic and are addressed through a standardization step described below. Let $X_1, X_2, \ldots, X_N$ be an independent random sample drawn from an absolutely continuous distribution with cumulative distribution function F, and let $X_{1:N} \leq X_{2:N} \leq \cdots \leq X_{N:N}$ denote the corresponding order statistics. The objective is to test whether the underlying distribution is symmetric about an unknown center μ. Formally, we consider the hypotheses

$$\mathcal{H}_0: F(\mu+x)=1-F(\mu-x), \text{ for all } x \in S_X$$

against

$$\mathcal{H}_1: F(\mu+x) \neq 1-F(\mu-x), \text{ for all } x \in S_X.$$

The proposed test exploits the equality of extropy- and cumulative -extropy-based measures associated with consecutive systems under symmetry. Departures from symmetry are detected through discrepancies between their empirical counterparts, yielding a test procedure that does not rely on moment conditions or parametric assumptions. To operationalize the proposed test, we construct a symmetry-sensitive statistic based on the extropy characterizations derived in (12) and (13).

For clarity and ease of application, the proposed testing procedure can be summarized as follows. First, the observed sample is standardized using the sample standard deviation to account for scale

effects. Next, an appropriate window parameter m is selected as a function of the sample size. The test statistic is then computed based on the empirical spacing representation derived in this section. Finally, the computed value is compared with the corresponding Monte Carlo critical values. The null hypothesis of symmetry is rejected when the statistic falls in the rejection region. This concise implementation highlights the simplicity, robustness, and practical applicability of the proposed symmetry test in real data settings.

Specifically, for integers $n \geq 2r$, we define

$$\mathcal{X}_{r,n} = \mathcal{J}(T_{n-r|n:G}) - \mathcal{J}(T_{n-r|n:F}),$$

which measures the difference between the extropies of the associated consecutive $(n-r)$-out-of-n:G and $(n-r)$-out-of-n:F systems. Using the representation in (12), this quantity can be expressed as:

$$\mathcal{X}_{r,n} = \frac{1}{2}\int_0^1 \left[\rho^2_{n-r|n:F}(u) - \rho^2_{n-r|n:G}(u)\right] f(F^{-1}(u))du$$

or, equivalently,

$$\mathcal{X}_{r,n} = \tfrac{1}{2}\textstyle\int_0^1 \left[\rho^2_{n-r|n:F}(u) - \rho^2_{n-r|n:G}(u)\right]\left[\frac{dF^{-1}(u)}{du}\right]^{-1} du. \tag{24}$$

In practice, the derivative $dF^{-1}(u)/du$ is unknown and must be estimated from the data. Following Vasicek [27], we approximate this quantity using a finite-difference scheme based on the empirical distribution function. This leads to the following plug-in estimator:

$$\widehat{\mathcal{X}}_{r,n} = \tfrac{1}{2N}\textstyle\sum_{k=1}^{N} \left[\rho^2_{n-r|n:F}\left(\frac{k}{N+1}\right) - \rho^2_{n-r|n:G}\left(\frac{k}{N+1}\right)\right]\left[\frac{2m}{N(X_{k+m:N}-X_{k-m:N})}\right], \tag{25}$$

which is valid for $n \geq 2r$. Here, $m < N/2$ denotes a smoothing (window) parameter that controls the bias–variance trade-off of the estimator. To address boundary effects, we set $X_{k-m:N} = X_{1:N}$ whenever $k - m \leq 1$ and $X_{k+m:N} = X_{N:N}$ whenever $k + m \geq N$. Under the null hypothesis of symmetry, the statistic $\widehat{\mathcal{X}}_{r,n}$ is expected to be close to zero, whereas substantial positive or negative values indicate departures from symmetry. As with any inferential procedure, the performance of the proposed test depends critically on the large-sample behavior of the estimator. The nonparametric estimator considered here is related to efficient distribution-free estimation procedures; see, for example, the recent ranked set sampling approach proposed in Li and Chen [28].

The finite-sample null distribution of the statistic $\widehat{\mathcal{X}}_{r,n}$ is analytically intractable due to its dependence on order statistics and local spacing estimators. In the original implementation, critical values were obtained via Monte Carlo simulation using a symmetric case of the generalized lambda distribution (GLD). This choice was motivated by the flexibility of the GLD family, which can approximate a wide range of symmetric distributional shapes through its quantile-based formulation. To assess the robustness of this calibration beyond a single null model, we conducted additional Monte Carlo experiments under several commonly used symmetric distributions, including the normal, Laplace, logistic, Student-t (with varying degrees of freedom), the uniform distribution, and Cauchy distributions. Across all considered null models, the empirical rejection rates remained close to the nominal significance levels, indicating that the proposed calibration provides adequate size control under symmetry. These results suggest that the GLD-based calibration serves as a convenient representative symmetric null rather than a restrictive assumption. We note that alternative data-driven calibration methods, such as reflection-based bootstrap or permutation procedures tailored to

symmetry, may also be employed if desired. However, the simulation results indicate that the proposed approach achieves reliable size control across a broad class of symmetric distributions.

The consistency of $\widehat{\mathcal{X}}_{r,n}$ is established in the following theorem.

Theorem 5.1. Let $X_1, X_2, \ldots, X_N$ be a random sample of size N from a population with probability density function f and a cumulative distribution function F and finite variance. Then, as $N \to +\infty, m \to +\infty$, and $m/N \to 0, \widehat{\mathcal{X}}_{r,n} \xrightarrow{p} \mathcal{X}_{r,n}$, where $\xrightarrow{p}$ denotes convergence in probability.

Proof. To establish the consistency of the estimator $\widehat{\mathcal{X}}_{r,n}$, we follow the methodology introduced by Noughabi and Arghami [29]. Consider a sequence in which both the sample size N and the window parameter m tend to infinity while the ratio $m/N \to 0$. Under this asymptotic regime, the finite-difference term in the estimator can be interpreted as a local density approximation. Specifically,

$$\begin{aligned}\frac{2m}{N(X_{k+m:N} - X_{k-m:N})} &= \frac{F_N(X_{k+m:N}) - F_N(X_{k-m:N})}{X_{k+m:N} - X_{k-m:N}} \\ &\approx \frac{F(X_{k+m:N}) - F(X_{k-m:N})}{X_{k+m:N} - X_{k-m:N}} \\ &= \frac{f(X_{k+m:N}) - f(X_{k-m:N})}{2} \simeq f(X_{k:N}),\end{aligned}$$

where F_N represents the empirical distribution function. Recall that $F_N(X_{k:N}) = \mathrm{k}/(\mathrm{N}+1)$. Substituting this into the definition of $\widehat{\mathcal{X}}_{r,n}$, we obtain

$$\begin{aligned}\widehat{\mathcal{X}}_{r,n} &= \frac{1}{2N}\sum_{k=1}^{N}\left(\rho^2_{n-r|n:F}\left(\frac{k}{N+1}\right) - \rho^2_{n-r|n:G}\left(\frac{k}{N+1}\right)\right)\left(\frac{2m}{N(X_{k+m:N} - X_{k-m:N})}\right) \\ &\simeq \frac{1}{2N}\sum_{k=1}^{N}\left(\rho^2_{n-r|n:F}\left(F_N(X_{k:N})\right) - \rho^2_{n-r|n:G}\left(F_N(X_{k:N})\right)\right) f(X_{k:N}) \\ &= \frac{1}{2N}\sum_{k=1}^{N}\left(\rho^2_{n-r|n:F}\left(F(X_{k:N})\right) - \rho^2_{n-r|n:G}\left(F(X_{k:N})\right)\right) f(X_{k:N}) \\ &= \frac{1}{2N}\sum_{k=1}^{N}\left(\rho^2_{n-r|n:F}\left(F(X_k)\right) - \rho^2_{n-r|n:G}\left(F(X_k)\right)\right) f(X_k).\end{aligned}$$

Using the almost sure uniform convergence of the empirical distribution function $F_N(X_{k:N}) \xrightarrow{\text{a.s.}} F(X_{k:N})$ as $N \to \infty$ and the continuity of the functions $\rho^2_{n-r|n:F}$ and $\rho^2_{n-r|n:G}$, it follows that

$$\begin{aligned}\widehat{\mathcal{X}}_{r,n} &\xrightarrow{\text{a.s.}} \frac{1}{2N}\sum_{k=1}^{N}\left(\rho^2_{n-r|n:F}\left(F(X_{k:N})\right) - \rho^2_{n-r|n:G}\left(F(X_{k:N})\right)\right) f(X_{k:N}) \\ &= \frac{1}{2N}\sum_{k=1}^{N}\left(\rho^2_{n-r|n:F}\left(F(X_k)\right) - \rho^2_{n-r|n:G}\left(F(X_k)\right)\right) f(X_k)\end{aligned}$$

as $N \to \infty$. Now, observe that the right-hand side is a sample average of the form

$$\tfrac{1}{N}\textstyle\sum_{k=1}^{N} Z_k, \text{ where } Z_k = \frac{1}{2}\left[\left(\rho^2_{n-r|n:F}\left(F(X_k)\right) - \rho^2_{n-r|n:G}\left(F(X_k)\right)\right) f(X_k)\right].$$

Now, the strong law of large numbers yields

$$\begin{aligned}\frac{1}{N}\sum_{k=1}^{N} Z_k &\xrightarrow{\text{a.s.}} E\left(\frac{1}{2}\left(\rho^2_{n-r|n:F}(F(X)) - \rho^2_{n-r|n:G}(F(X))\right)f(X)\right)\\ &= \frac{1}{2}\int_0^{\infty}\left(\rho^2_{n-r|n:F}(F(x)) - \rho^2_{n-r|n:G}(F(x))\right)f^2(x)dx\\ &= \mathcal{J}(T_{n-r|n:G}) - \mathcal{J}(T_{n-r|n:F}) = \mathcal{X}_{r,n}.\end{aligned}$$

Therefore $\widehat{\mathcal{X}}_{r,n} \xrightarrow{\text{a.s.}} \mathcal{X}_{r,n}$ as $m, N \to \infty$ and $m/N \to 0$, which establishes the strong consistency of the proposed estimator. This completes the proof of consistency.

The shift of a random variable X does not affect the variance of $\widehat{\mathcal{X}}_{r,n}$ when estimating $\mathcal{X}_{r,n}$, but this is not true for scale transformations. This result follows from the arguments in Ebrahimi et al. [30].

Theorem 5.2. Assume that $X_1, X_2, \ldots, X_N$ is a random sample of size N taken from a population with probability density function f and $CDFF$ and $Y_i = aX_i + b, a > 0, b \in R$. Denote the estimators for $\mathcal{X}_{r,n}$ on the basis of X_i and Y_i with $\widehat{\mathcal{X}}^X_{r,n}$ and $\widehat{\mathcal{X}}^Y_{r,n}$, respectively. Then, the following properties apply:
(i). $\mathbb{E}\left(\widehat{\mathcal{X}}^Y_{r,n}\right) = \mathbb{E}\left(\widehat{\mathcal{X}}^X_{r,n}\right)/a$,
(ii). $\mathrm{Var}\left(\widehat{\mathcal{X}}^Y_{r,n}\right) = \mathrm{Var}\left(\widehat{\mathcal{X}}^X_{r,n}\right)/a^2$.

Proof. Equation (25) shows that

$$\begin{aligned}\widehat{\mathcal{X}}^Y_{r,n} &= \frac{1}{2N}\sum_{k=1}^{N}\left(\rho^2_{n-r|n:F}\left(\frac{k}{N+1}\right) - \rho^2_{n-r|n:G}\left(\frac{k}{N+1}\right)\right)\frac{2m}{N(Y_{k+m:N} - Y_{k-m:N})}\\ &= \frac{1}{2N}\sum_{k=1}^{N}\left(\rho^2_{n-r|n:F}\left(\frac{k}{N+1}\right) - \rho^2_{n-r|n:G}\left(\frac{k}{N+1}\right)\right)\frac{2m}{aN(X_{k+m:N} - X_{k-m:N})}\\ &= \frac{\widehat{\mathcal{X}}^X_{r,n}}{a}.\end{aligned}$$

The proof concludes by using the mean and variance of $\widehat{\mathcal{X}}^Y_{r,n} = \widehat{\mathcal{X}}^X_{r,n}/a$. ■

As shown in Theorem 5.2, scale transformations affect the variance of the estimator $\widehat{\mathcal{X}}_{r,n}$, whereas location shifts do not. Accordingly, in all simulation studies and real-data applications reported in this paper, the observations are standardized by the sample standard deviation prior to computing the test statistic. This standardization ensures comparability across different scales and stabilizes the finite-sample behavior of the procedure. In practice, the recommended implementation is as follows: given a sample $X_1, X_2, \ldots, X_n$, the data may optionally be centered for numerical stability (although not required), standardized by the sample standard deviation, and then directly used to compute $\widehat{\mathcal{X}}_{r,n}$ with the chosen window parameter. For simplicity, we choose $r = 1$ and $n = 3$ as the minimal nontrivial configuration satisfying $n \geq 2r$, which balances sensitivity to asymmetry with computational tractability, and employ it in the following:

$$\widehat{\mathcal{X}}_{1,3} = \frac{1}{2N}\sum_{k=1}^{N}\left(\rho^2_{2|3:F}\left(\frac{k}{N+1}\right) - \rho^2_{2|3:G}\left(\frac{k}{N+1}\right)\right)\left(\frac{2m}{N(X_{k+m:N} - X_{k-m:N})}\right).$$

The symmetry of the distribution of X is assessed using the sample estimate $\widehat{\mathcal{X}}_{1,3} = \hat{\mathcal{J}}(T_{2|3:G}) - \hat{\mathcal{J}}(T_{2|3:F})$. We reject the assumption of symmetry when $\widehat{\mathcal{X}}_{1,3}$ is significantly small or large, as these

values suggest asymmetry of the distribution. Under the null hypothesis $H_0, \widehat{\mathcal{X}}_{1,3}$ converges to zero. Because the values of $\widehat{\mathcal{X}}_{1,3}$ depend on both the window size m and the sample and because deriving the exact null distribution of $\widehat{\mathcal{X}}_{1,3}$ is intractable, we use Monte Carlo simulation to estimate its critical values. To this aim, critical values are calculated using the first case of the GLD. A random variable X follows a GLD with parameters $\lambda_i, i = 1, 2, 3, 4$ if its quantile function is given by

$$F^{-1}(u) = \lambda_1 + \frac{u^{\lambda_3} - (1-u)^{\lambda_4}}{\lambda_2}, \text{for } 0 < u < 1.$$

The parameters λ_3 and λ_4 control skewness and kurtosis, λ_2 affects variance, and λ_1 determines the mean. The distribution is symmetric around λ_1 when $\lambda_3 = \lambda_4$. Table 1 presents nine commonly used GLD cases for evaluating symmetry tests; probability density function shapes are illustrated in Figure 4 of Amiri and Khaledi [31]. We reject the null hypothesis at significance level α for sample size N if $\left|\widehat{\mathcal{X}}_{1,3}\right| \geq \widehat{\mathcal{X}}_{1,3,(1-\alpha/2)}$. Because the distribution of $\widehat{\mathcal{X}}_{1,3}$ is complex and sensitive to N and the window parameter m, we used Monte Carlo simulation with 10,000 samples to determine critical values. Specifically, we generated samples of sizes $N = 5, 10, 20, 30, 40, 50, 100$ from the null distribution and estimated the $(1-\alpha/2)$th quantile. Tables 2 and 3 show critical values for $\alpha = 0.05, 0.01$ at various sample sizes.

Table 1. Nine cases of GLDs with k_3 and k_4 representing skewness and kurtosis, respectively.

Case	λ_1	λ_2	λ_3	λ_4	k_3	k_4
1	0.0000	0.1975	0.1349	0.1349	0.0000	3.0000
2	-0.1167	-0.3517	-0.1300	-0.1600	0.8000	11.4000
3	0.0000	-1.0000	-0.1000	-0.1800	2.0000	21.2000
4	3.5865	0.0431	0.0252	0.0940	0.9000	4.2000
5	0.0000	-1.0000	-0.0075	-0.0300	1.5000	7.5000
6	0.0000	1.0000	1.4000	0.2500	0.5000	2.2000
7	0.0000	1.0000	0.0001	0.1000	1.5000	5.8000
8	0.0000	-1.0000	-0.0010	-0.1300	3.1600	23.8000
9	0.0000	-1.0000	-0.0001	-0.1700	3.8800	40.7000

Table 2 reports the Monte Carlo-based critical values of the proposed test statistic $\widehat{\mathcal{X}}_{1,3}$ at the significance level α=0.05 for various sample sizes *N* and window parameters *m*. As expected, the critical values decrease as the sample size increases, reflecting the increasing concentration of the test statistic around its null value. For a fixed sample size, the critical values exhibit a mild dependence on the choice of *m*, indicating that the test is not overly sensitive to moderate changes in the window parameter. These critical values provide a practical reference for implementing the proposed symmetry test in finite samples.

Table 2. Critical values of the $\widehat{\mathcal{X}}_{1,3}$ statistic at $\alpha = 0.05$.

m	$N = 5$	$N = 10$	$N = 20$	$N = 30$	$N = 40$	$N = 50$	$N = 100$
2	0.490033	0.247000	0.100926	0.071244	0.059137	0.052337	0.035855
3		0.180701	0.083485	0.055663	0.045631	0.041415	0.028508
4		0.152703	0.079108	0.051461	0.041608	0.036205	0.025606
5		0.118496	0.081710	0.051614	0.039782	0.033406	0.024323
6			0.078248	0.052119	0.039387	0.033379	0.022832
7			0.077358	0.053082	0.039502	0.032339	0.022364
8			0.075081	0.052850	0.040221	0.033015	0.021387
9			0.070383	0.054158	0.040888	0.032348	0.020991
10			0.065407	0.055310	0.042017	0.033409	0.020367
11				0.054868	0.042925	0.034006	0.019974
12				0.055444	0.043562	0.036185	0.020101
13				0.054772	0.044529	0.036030	0.019526
14				0.053426	0.045276	0.036604	0.019666
15				0.049424	0.045284	0.037814	0.019563
16					0.044716	0.038320	0.019845
17					0.045902	0.039433	0.019745
18					0.045575	0.039922	0.020193
19					0.044759	0.039926	0.020140
20					0.04208	0.040505	0.020711
21						0.039442	0.020771
22						0.039463	0.021230
23						0.039802	0.021912
24						0.038844	0.021800
25						0.038413	0.022951
26							0.023710
27							0.023511
28							0.023972
29							0.024752
30							0.024911

Table 3 presents the corresponding Monte Carlo critical values of the statistic $\widehat{\mathcal{X}}_{1,3}$ at the more stringent significance level α=0.01. Compared with Table 2, the critical values are uniformly larger, as expected for a smaller significance level. The same general patterns are observed: critical values decrease with increasing sample size and vary moderately with the window parameter m. This table complements Table 2 by enabling practitioners to apply the proposed test at a stricter confidence level while maintaining consistency with the finite-sample calibration strategy. The performance of the proposed spacing-based symmetry test depends on the choice of the window parameter. We adopt a simple and widely used data-driven guideline by selecting the window parameter as a function of the sample size. This choice reflects a practical bias–variance trade-off commonly encountered in spacing-type estimators. The window parameter controls the classical trade-off inherent in spacing-based density approximations. Choosing a small window typically reduces smoothing bias but increases variability, whereas larger windows stabilize the estimate at the expense of potentially masking local asymmetry. The adopted rule therefore aims to maintain sufficient sensitivity to departures from

symmetry while keeping the estimator numerically stable, a compromise that is confirmed by the Monte Carlo evidence reported in this section. To assess robustness, we conducted additional numerical checks (not reported for brevity) indicating that the empirical size and power of the proposed test remain stable for moderate deviations around the chosen rule. Consequently, the test is not overly sensitive to the exact choice of the window parameter, and the proposed guideline provides a reliable and practical default for implementation.

Table 3. Critical values of the $\widehat{\mathcal{X}}_{1,3}$ statistic at $\alpha = 0.01$.

m	$N = 5$	$N = 10$	$N = 20$	$N = 30$	$N = 40$	$N = 50$	$N = 100$
2	1.112735	0.515603	0.183951	0.122031	0.090898	0.078790	0.053072
3		0.336872	0.132772	0.085135	0.069912	0.059402	0.041505
4		0.261805	0.122095	0.079105	0.061360	0.052073	0.035605
5		0.199821	0.129754	0.078275	0.057755	0.049450	0.033135
6			0.115798	0.076426	0.057054	0.045416	0.031934
7			0.112502	0.075993	0.056528	0.045089	0.030002
8			0.110428	0.080563	0.056582	0.048604	0.029127
9			0.103464	0.077802	0.059365	0.045029	0.029099
10			0.097427	0.079682	0.060474	0.048714	0.027372
11				0.081618	0.059550	0.046802	0.027865
12				0.075034	0.064334	0.050625	0.026880
13				0.078713	0.063218	0.049701	0.026858
14				0.076863	0.060808	0.053181	0.026419
15				0.069460	0.062473	0.051823	0.026610
16					0.062286	0.054119	0.027206
17					0.063533	0.053117	0.026887
18					0.062680	0.052579	0.027575
19					0.059284	0.054598	0.028128
20					0.059574	0.054983	0.028795
21						0.054226	0.028633
22						0.054277	0.029421
23						0.054395	0.029295
24						0.051512	0.029713
25						0.052672	0.030140
26							0.032572
27							0.031619
28							0.032612
29							0.032751
30							0.032897

5.1. Power comparisons

We evaluate the performance of the proposed symmetry test based on the statistic $\widehat{\mathcal{X}}_{1,3}$ by comparing it with a set of established symmetry tests listed in Table 4. The assessment focuses on empirical power against asymmetric alternatives generated from the GLD family, which provides a flexible framework for modeling a wide range of skewness patterns. In total, the proposed test is

benchmarked against ten existing symmetry tests. Power estimates are computed using the nine distributions reported in Table 1. The window size is selected as $m = \lfloor N/2 \rfloor - 1$, which was found to provide robust sensitivity across different degrees of asymmetry. For each sample size $N \in \{20, 30, 50, 100\}$, independent Monte Carlo replications are generated to approximate the empirical power of each test. In all Monte Carlo experiments, samples of sizes n∈{20, 30, 50, 100} were generated, and the window parameter was fixed at $m = \sqrt{n}$, which was found to provide a good balance between bias and variance in preliminary investigations. The critical values were obtained using Monte Carlo calibration under the symmetric Case 1 of the GLD, as described in Section 5.

Table 4. Symmetry tests.

Test	Reference	Notation
1	McWilliams [32]	R
2	Baklizi [33]	R_B
3	Gibbons and Chakraborti [34]	W
4	Tajuddin [35]	T
5	Cheng and Balakrishnan [36]	C_6
6	Modarres and Gastwirth [37]	M_p
7	Baklizi [38]	$L^{\star}_{n,0.8}$
8	Baklizi [39]	R_M
9	Corzo and Babativa [40]	J_6
10	Xiong et al. [3]	$\widehat{D}_2$

The empirical power is computed as the proportion of replications in which the null hypothesis of symmetry is rejected at the nominal significance level $\alpha = 0.05$. The resulting power estimates are reported in Table 5. Under the symmetric null model (Case 1 in Table 1), all tests, including the proposed procedure, exhibit empirical sizes close to the nominal level, confirming appropriate size control. For the asymmetric alternatives, particularly Cases 2 and 3 corresponding to mild or near-symmetric departures, the proposed test generally achieves competitive and often superior power compared with existing methods, with the exception of the variant $\widehat{D}_2$. These results indicate that the proposed procedure is especially effective in detecting subtle deviations from symmetry, suggesting clear practical advantages in applications where mild asymmetry is of primary concern.

Table 5. Empirical powers for the GLD with $\alpha = 0.05$.

Case	N	R	R_B	W	T	C_6	$M_{0.2}$	$M_{0.6}$	$L^{\star}_{n,0.8}$	R_M	J_6	$\widehat{D}_2$	$\widehat{\mathcal{X}}_{1,3}$
1	20	0.048	0.052	0.046	0.046	0.047	0.046	0.045	0.055	0.045	0.056	0.048	0.051
	30	0.050	0.053	0.052	0.050	0.052	0.050	0.054	0.054	0.045	0.047	0.049	0.043
	50	0.050	0.054	0.050	0.052	0.050	0.050	0.049	0.050	0.050	0.046	0.051	0.049
	100	0.051	0.047	0.052	0.048	0.052	0.053	0.051	0.054	0.051	0.048	0.049	0.059
2	20	0.052	0.057	0.050	0.051	0.054	0.053	0.053	0.062	0.058	0.070	0.092	0.183
	30	0.052	0.051	0.055	0.056	0.061	0.053	0.055	0.063	0.062	0.061	0.095	0.212
	50	0.055	0.056	0.052	0.060	0.070	0.063	0.066	0.062	0.075	0.068	0.119	0.266
	100	0.054	0.051	0.055	0.071	0.091	0.057	0.062	0.066	0.106	0.084	0.151	0.343
3	20	0.067	0.075	0.055	0.079	0.080	0.077	0.087	0.088	0.114	0.112	0.604	0.743
	30	0.074	0.075	0.062	0.097	0.119	0.092	0.109	0.128	0.156	0.125	0.664	0.781
	50	0.089	0.094	0.064	0.131	0.204	0.121	0.153	0.145	0.253	0.206	0.773	0.845
	100	0.113	0.109	0.088	0.224	0.366	0.169	0.217	0.228	0.486	0.356	0.897	0.903
4	20	0.090	0.103	0.061	0.106	0.118	0.120	0.142	0.138	0.187	0.177	0.017	0.008
	30	0.114	0.122	0.070	0.149	0.219	0.163	0.199	0.229	0.287	0.243	0.022	0.009
	50	0.143	0.154	0.085	0.209	0.428	0.231	0.301	0.303	0.499	0.443	0.035	0.023
	100	0.216	0.209	0.127	0.385	0.757	0.398	0.522	0.572	0.818	0.750	0.135	0.105
5	20	0.115	0.131	0.067	0.133	0.155	0.158	0.190	0.165	0.254	0.235	0.982	0.986
	30	0.151	0.160	0.080	0.194	0.309	0.228	0.287	0.333	0.404	0.343	0.991	0.994
	50	0.197	0.213	0.103	0.287	0.587	0.338	0.437	0.457	0.668	0.602	0.998	0.997
	100	0.321	0.316	0.166	0.522	0.890	0.555	0.696	0.769	0.939	0.885	1.000	0.999
6	20	0.200	0.234	0.072	0.160	0.256	0.334	0.396	0.267	0.420	0.468	0.803	0.704
	30	0.303	0.330	0.095	0.231	0.606	0.546	0.671	0.649	0.653	0.715	0.929	0.848
	50	0.497	0.524	0.122	0.364	0.950	0.815	0.920	0.908	0.894	0.972	0.991	0.961
	100	0.782	0.782	0.198	0.633	1.000	0.986	0.998	1.000	0.994	1.000	1.000	0.999
7	20	0.311	0.358	0.096	0.281	0.421	0.496	0.578	0.330	0.593	0.644	0.999	0.995
	30	0.457	0.490	0.123	0.393	0.797	0.737	0.828	0.823	0.854	0.868	1.000	0.999
	50	0.683	0.707	0.185	0.600	0.991	0.937	0.977	0.978	0.980	0.994	1.000	1.000
	100	0.928	0.927	0.358	0.883	1.000	0.999	1.000	1.000	1.000	1.000	1.000	1.000
8	20	0.373	0.426	0.105	0.330	0.494	0.581	0.656	0.366	0.666	0.715	0.998	0.998
	30	0.539	0.570	0.150	0.484	0.861	0.810	0.878	0.876	0.913	0.915	1.000	1.000
	50	0.761	0.782	0.233	0.697	0.996	0.967	0.989	0.991	0.993	0.998	1.000	1.000
	100	0.966	0.965	0.420	0.947	1.000	1.000	1.000	1.000	1.000	1.000	1.000	1.000
9	20	0.399	0.452	0.112	0.351	0.530	0.618	0.696	0.359	0.692	0.752	1.000	0.999
	30	0.580	0.614	0.152	0.498	0.877	0.841	0.900	0.898	0.924	0.929	1.000	0.999
	50	0.802	0.821	0.241	0.725	0.997	0.977	0.992	0.993	0.995	0.999	1.000	1.000
	100	0.980	0.980	0.441	0.956	1.000	1.000	1.000	1.000	1.000	1.000	1.000	1.000

5.2. Real dataset

To further demonstrate the practical applicability of the proposed symmetry test, we analyze two real datasets drawn from the literature. The first dataset, originally reported by Qiu and Jia [41], is well fitted by an asymmetric inverse Gaussian distribution and is used to illustrate the operational performance of the proposed test statistic. The second dataset, taken from Lawless [42], follows an

asymmetric Chen distribution and serves to highlight the comparative effectiveness of our approach. For each dataset, we compute the p-value of the proposed test statistic $\widehat{\mathcal{X}}_{1,3}$ and compare it with those obtained from several classical symmetry tests that are widely implemented in standard statistical software. All tests are conducted at the 5% significance level. This comparative analysis provides empirical evidence of the ability of the proposed procedure to detect asymmetry in real-world data settings.

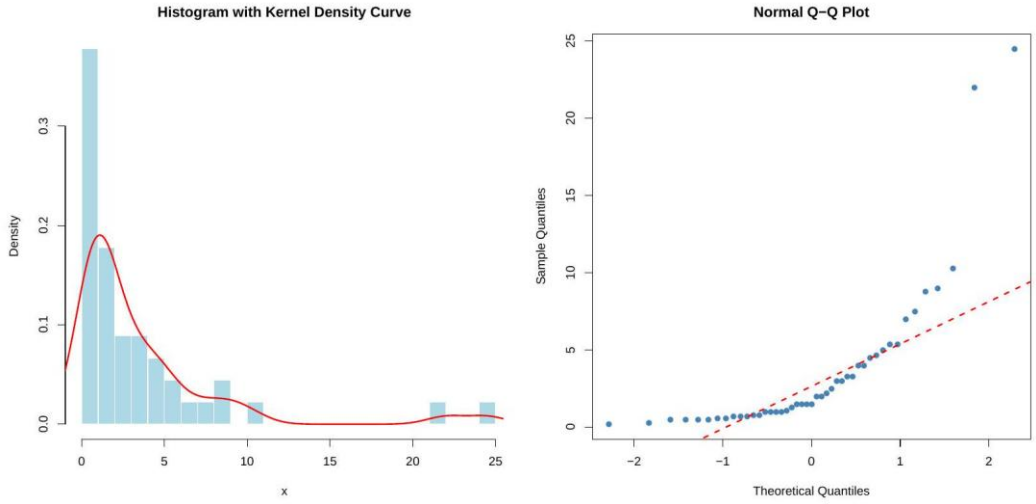

Figure 2. Histogram with kernel density estimate and Q–Q plot for the data in Example 5.1.

For each real dataset, the proposed symmetry test was applied after standardizing the observations by the sample standard deviation. The window parameter was selected as $m = \sqrt{n}$, where n denotes the sample size. The corresponding p-values were computed using the GLD-based Monte Carlo calibration described in Section 5.

Example 5.1. Let us consider the airborne communication transceiver repair time dataset, which follows an asymmetric inverse Gaussian distribution. This dataset, originally presented in Qiu and Jia [41], serves to illustrate the functionality of our test statistic.

Dataset: 0.2, 0.3, 0.5, 0.5, 0.5, 0.5, 0.6, 0.6, 0.7, 0.7, 0.7, 0.8, 0.8, 1.0, 1.0, 1.0, 1.0, 1.1, 1.3, 1.5, 1.5, 1.5, 1.5, 2.0, 2.0, 2.2, 2.5, 3.0, 3.0, 3.3, 3.3, 4.0, 4.0, 4.5, 4.7, 5.0, 5.4, 5.4, 7.0, 7.5, 8.8, 9.0, 10.3, 22.0, 24.5.

Figure 2 displays the histogram with the corresponding kernel density estimate along with the Q–Q plot of the data. The dataset exhibits pronounced right skewness, with an estimated skewness of 2.848 and kurtosis of 8.5171, which indicate substantial deviation from symmetry. Applying the proposed symmetry test with sample size $N = 45$ and window parameter $m = 22$ yields a test statistic $\left|\widehat{\mathcal{X}}_{1,3}\right| = 0.064$, corresponding to a p-value of 0.004. This result provides strong evidence against the null hypothesis of symmetry, thereby confirming the presence of asymmetry in the underlying distribution.

Example 5.2. Here, we consider the data from Cobb [43] below, which includes observations of the Nile River's yearly flow at Aswan between 1871 and 1970 as follows:

Dataset: 1120, 1160, 963, 1210, 1160, 1160, 813, 1230, 1370, 1140, 995, 935, 1110, 994, 1020,

960, 1180, 799, 958, 1140, 1100, 1210, 1150, 1250, 1260, 1220, 1030, 1100, 774, 840, 874, 694, 940, 833, 701, 916, 692, 1020, 1050, 969, 831, 726, 456, 824, 702, 1120, 1100, 832, 764, 821, 768, 845, 864, 862, 698, 845, 744, 796, 1040, 759, 781, 865, 845, 944, 984, 897, 822, 1010, 771, 676, 649, 846, 812, 742, 801, 1040, 860, 874, 848, 890, 744, 749, 838, 1050, 918, 986, 797, 923, 975, 815, 1020, 906, 901, 1170, 912, 746, 919, 718, 714, 740.

The data exhibit approximately symmetric behavior, with an estimated skewness of 0.322 and kurtosis of 2.695, both indicating only mild departures from normality. Figure 3 presents the histogram with the corresponding kernel density estimate, together with the Q–Q plot. Applying the proposed symmetry test with sample size $N = 100$ and window parameter $m = 49$ yields a test statistic $|\hat{\mathcal{X}}_{1,3}|$ that is close to zero, resulting in a nonsignificant p-value at the 5% level. Consequently, there is no evidence to reject the null hypothesis of symmetry, which is consistent with the descriptive characteristics of the data.

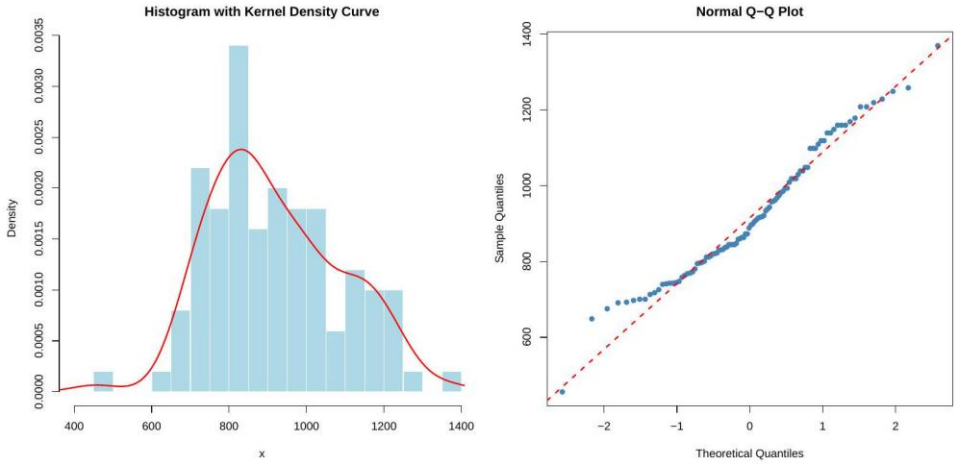

Figure 3. Histogram with kernel density estimate and Q–Q plot for the data in Example 5.2.

6. Conclusions

Symmetry plays a fundamental role in statistical modeling and inference, underpinning a wide range of applications in finance, engineering, physics, and data science. Assessing symmetry is therefore not only of theoretical interest but also of practical importance, particularly in nonparametric settings where model assumptions must be carefully validated. In this paper, we developed a unified information-theoretic framework for characterizing symmetric distributions through extropy-based measures, including differential extropy, cumulative residual extropy, and cumulative past extropy, within the context of consecutive reliability systems. By exploiting the structural properties of $(n-r)$-out-of-n:G and $(n-r)$-out-of-n:F systems, we established necessary and sufficient conditions under which equality of these extropy measures characterizes distributional symmetry. These results provide new insights into the interplay between information measures and system-based representations of random variables. Building upon the theoretical characterizations, we proposed a new nonparametric test for symmetry based on differences in estimated extropies of consecutive systems. The test was shown to be consistent, and extensive Monte Carlo simulations demonstrated that it exhibits competitive and often superior power compared to several existing symmetry tests, particularly in detecting mild or near-symmetric departures, which are notoriously challenging in practice. Applications to real datasets further confirmed the practical relevance and interpretability of

the proposed methodology. Overall, this work bridges reliability theory, information theory, and nonparametric statistical inference, offering both rigorous characterization results and a practically implementable testing procedure. Potential extensions of the proposed methodology include multivariate distributional settings and the incorporation of alternative information measures, which constitute promising directions for future research. The results presented in this study naturally suggest several promising directions for future research:

(1) The current framework assumes independent observations. Extending extropy-based symmetry characterizations and tests to dependent structures such as time series, spatial data, or copula-based models, would significantly broaden applicability.

(2) An important avenue is the development of extropy-based characterizations and tests for multivariate symmetry, including elliptical and centrally symmetric distributions, possibly via multivariate consecutive systems or depth-based extensions.

(3) Investigating robust versions of the proposed estimators as well as data-driven selection of the window parameter m could further improve finite-sample performance, particularly in the presence of outliers or heavy-tailed distributions.

(4) The methodology may be extended by incorporating generalized information measures, such as Rényi extropy, Tsallis extropy, or cumulative fractional extropies, allowing finer sensitivity control under different distributional regimes.

(5) Given the system-based formulation, further applications in reliability engineering, survival analysis, and maintenance modeling, especially under censoring or competing risks, constitute a natural and impactful extension.

Author contributions

The authors declare that they have contributed equally to the conception, design, analysis, and writing of this manuscript. All authors read and approved the final manuscript.

Use of Generative-AI tools declaration

The authors declare that no generative AI tools were used in the writing or analysis of this manuscript.

Acknowledgments

The authors would like to thank the four anonymous reviewers for their careful reading of the manuscript and for their constructive comments, which greatly improved the clarity and quality of the paper. This work is supported by the Ongoing Research Funding program, (ORF-2026-392), King Saud University, Riyadh, Saudi Arabia.

Conflict of interest

The authors declare that they have no conflicts of interest.

Abbreviations

CREX	Cumulative residual extropy
CPEX	Cumulative past extropy
X	Absolutely continuous random variable
$X_{(i)}$	(i)-th order statistic
F, f	Distribution function and density of (X)
Q	Quantile function associated with (F)
m	Window parameter used in spacing-based estimation
$\lfloor \cdot \rfloor$	Floor function
Ω	Support of the distribution

References

1. C. E. Shannon, A mathematical theory of communication, *Bell Syst. Tech. J.*, **27** (1948), 623–656. https://doi.org/10.1002/j.1538-7305.1948.tb00917.x
2. F. Lad, G. Sanfilippo, G. Agro, Extropy: complementary dual of entropy, *Statist. Sci.*, **30** (2015), 40–58. https://doi.org/10.1214/14-sts430
3. P. Xiong, W. Zhuang, G. Qiu, Testing symmetry based on the extropy of record values, *J. Nonparametr. Stat.*, **33** (2021), 134–155. https://doi.org/10.1080/10485252.2021.1914338
4. M. Z. Raqab, G. Qiu, On extropy properties of ranked set sampling, *Statistics*, **53** (2019), 210–226. https://doi.org/10.1080/02331888.2018.1533963
5. J. Jose, E. I. A. Sathar, Symmetry being tested through simultaneous application of upper and lower k-records in extropy, *J. Stat. Comput. Simul.*, **92** (2022), 830–846. https://doi.org/10.1080/00949655.2021.1975283
6. N. Gupta, S. K. Chaudhary, Some characterizations of continuous symmetric distributions based on extropy of record values, *Stat. Papers*, **65** (2024), 291–308. https://doi.org/10.1007/s00362-022-01392-y
7. S. M. A. Jahanshahi, H. Zarei, A. H. Khammar, On cumulative residual extropy, *Probab. Eng. Inf. Sci.*, **34** (2020), 605–625. https://doi.org/10.1017/s0269964819000196
8. K. H. Jung, H. Kim, Linear consecutive-k-out-of-n: F system reliability with common-mode forced outages, *Reliab. Eng. Syst. Safety*, **41** (1993), 49–55. https://doi.org/10.1016/0951-8320(93)90017-s
9. J. Shen, M. J. Zuo, Optimal design of series consecutive-k-out-of-n: G systems, *Reliab. Eng. Syst. Safety*, **45** (1994), 277–283. https://doi.org/10.1016/0951-8320(94)90144-9
10. W. Kuo, M. J. Zuo, *Optimal reliability modeling: principles and applications*, John Wiley and Sons, New York, 2003
11. S. Eryilmaz, Reliability properties of consecutive k-out-of-n systems of arbitrarily dependent components, *Reliab. Eng. Syst. Safety*, **94** (2009), 350–356. https://doi.org/10.1016/j.ress.2008.03.027
12. J. Honerkamp, *Statistical physics: an advanced approach with applications*, Springer, New York, 2012. https://doi.org/10.1007/978-3-642-28684-1

13. M. Mahdizadeh, E. Zamanzade, Estimation of a symmetric distribution function in multistage ranked set sampling, *Stat. Papers*, **61** (2020), 851–867. https://doi.org/10.1007/s00362-017-0965-x
14. M. Fashandi, J. Ahmadi, Characterizations of symmetric distributions based on Rényi entropy, *Stat. Probab. Lett.*, **82** (2012), 798–804. https://doi.org/10.1016/j.spl.2012.01.004
15. N. Balakrishnan, A. Selvitella, Symmetry of a distribution via symmetry of order statistics, *Stat. Probab. Lett.*, **129** (2017), 367–372. https://doi.org/10.1016/j.spl.2017.06.023
16. J. Ahmadi, M. Fashandi, Characterization of symmetric distributions based on some information measure properties of order statistics, *Phys. A*, **517** (2019), 141–152. https://doi.org/10.1016/j.physa.2018.11.009
17. M. Kayid, M. Shrahili, Information properties of consecutive systems using fractional generalized cumulative residual entropy, *Fractal Fract.*, **8** (2024), 568. https://doi.org/10.3390/fractalfract8100568
18. M. Kayid, M. A. Alshehri, Shannon differential entropy properties of consecutive k-out-of-n: G systems, *Oper. Res. Lett.*, **57** (2024), 107190. https://doi.org/10.1016/j.orl.2024.107190
19. U. Kamps, Characterizations of distributions by recurrence relations and identities for moments of order statistics, In: N. Balakrishnan, C. R. Rao, *Handbook of statistics*, Elsevier, **16** (1998), 291–311. https://doi.org/10.1016/s0169-7161(98)16012-1
20. J. S. Hwang, G. D. Lin, On a generalized moment problem II, *Proc. Amer. Math. Soc.*, **91** (1984), 577–580. https://doi.org/10.2307/2044804
21. F. Alrewely, M. Kayid, Extropy analysis in consecutive r-out-of-n: G systems with applications in reliability and exponentiality testing, *AIMS Math.*, **10** (2025), 6040–6068. https://doi.org/10.3934/math.2025276
22. G. Alomani, F. Alrewely, M. Kayid, Information-theoretic reliability analysis of linear consecutive r-out-of-n: F systems and uniformity testing, *Entropy*, **27** (2025), 590. https://doi.org/10.3390/e27060590
23. M. A. Kon, *Probability distributions in quantum statistical mechanics*, Springer, New York, 1985. https://doi.org/10.1007/BFb0077154
24. J. Naudts, *Generalised thermostatistics*, Springer, New York, 2011. https://doi.org/10.1007/978-0-85729-355-8
25. S. Sirca, *Probability for physicists*, Springer, New York, 2016. https://doi.org/10.1007/978-3-319-31611-6.
26. J. Ahmadi, Characterization results for symmetric continuous distributions based on the properties of k-records and spacings, *Stat. Probab. Lett.*, **162** (2020), 108764. https://doi.org/10.1016/j.spl.2020.108764
27. O. Vasicek, A test for normality based on sample entropy, *J. R. Stat. Soc., Ser. B*, **38** (1976), 54–59. https://doi.org/10.1111/j.2517-6161.1976.tb01566.x
28. M. Li, W. Chen, 3 × 3 optimal ranked set sampling design with cycles and best linear invariant estimators of the parameters for normal distribution, *Stat. Probab. Lett.*, **224** (2025), 110455. https://doi.org/10.1016/j.spl.2025.110455
29. H. A. Noughabi, N. R. Arghami, Testing exponentiality based on characterizations of the exponential distribution, *J. Stat. Comput. Simul.*, **81** (2011), 1641–1651. https://doi.org/10.1080/00949655.2010.498373
30. N. Ebrahimi, K. Pflughoeft, E. S. Soofi, Two measures of sample entropy, *Stat. Probab. Lett.*, **20** (1994), 225–234. https://doi.org/10.1016/0167-7152(94)90046-9

31. M. Amiri, B. E. Khaledi, A new test for symmetry against right skewness, *J. Stat. Comput. Simul.*, **86** (2016), 1479–1496. https://doi.org/10.1080/00949655.2015.1071374
32. T. P. McWilliams, A distribution-free test for symmetry based on a runs statistic, *J. Amer. Stat. Assoc.*, **85** (1990), 1130–1133. https://doi.org/10.1080/01621459.1990.10474985
33. A. Baklizi, A conditional distribution-free runs test for symmetry, *J. Nonparametr. Stat.*, **15** (2003), 713–718. https://doi.org/10.1080/10485250310001634737
34. J. D. Gibbons, S. Chakraborti, *Nonparametric statistical inference*, Marcel Dekker, New York, 1992.
35. I. H. Tajuddin, Distribution-free test for symmetry based on Wilcoxon two-sample test, *J. Appl. Stat.*, **21** (1994), 409–415. https://doi.org/10.1080/757584017
36. W. H. Cheng, N. Balakrishnan, A modified sign test for symmetry, *Commun. Stat.—Simul. Comput.*, **33** (2004), 703–709. https://doi.org/10.1081/sac-200033302
37. R. Modarres, J. L. Gastwirth, Hybrid test for the hypothesis of symmetry, *J. Appl. Stat.*, **25** (1998), 777–783. https://doi.org/10.1080/02664769822765
38. A. Baklizi, Testing symmetry using a trimmed longest run statistic, *Aust. NZ J. Stat.*, **49** (2007), 339–347. https://doi.org/10.1111/j.1467-842x.2007.00485.x
39. A. Baklizi, Improving the power of the hybrid test of symmetry, *Int. J. Contemp. Math. Sci.*, **3** (2008), 497–499.
40. J. Corzo, G. Babativa, A modified runs test for symmetry, *J. Stat. Comput. Simul.*, **83** (2013), 984–991. https://doi.org/10.1080/00949655.2011.647026
41. G. Qiu, K. Jia, Extropy estimators with applications in testing uniformity, *J. Nonparametr. Stat.*, **30** (2018), 182–196. https://doi.org/10.1080/10485252.2017.1404063
42. J. F. Lawless, *Statistical models and methods for lifetime data*, John Wiley and Sons, New York, 2011.
43. G. W. Cobb, The problem of the Nile: Conditional solution to a changepoint problem, *Biometrika*, **65** (1978), 243–251. https://doi.org/10.2307/2335202

AIMS Press